Introduction to GW data analysis
Part I

Frédérique Marion

4th MaNiTou Summer School on Gravitational Waves

2025

Scope

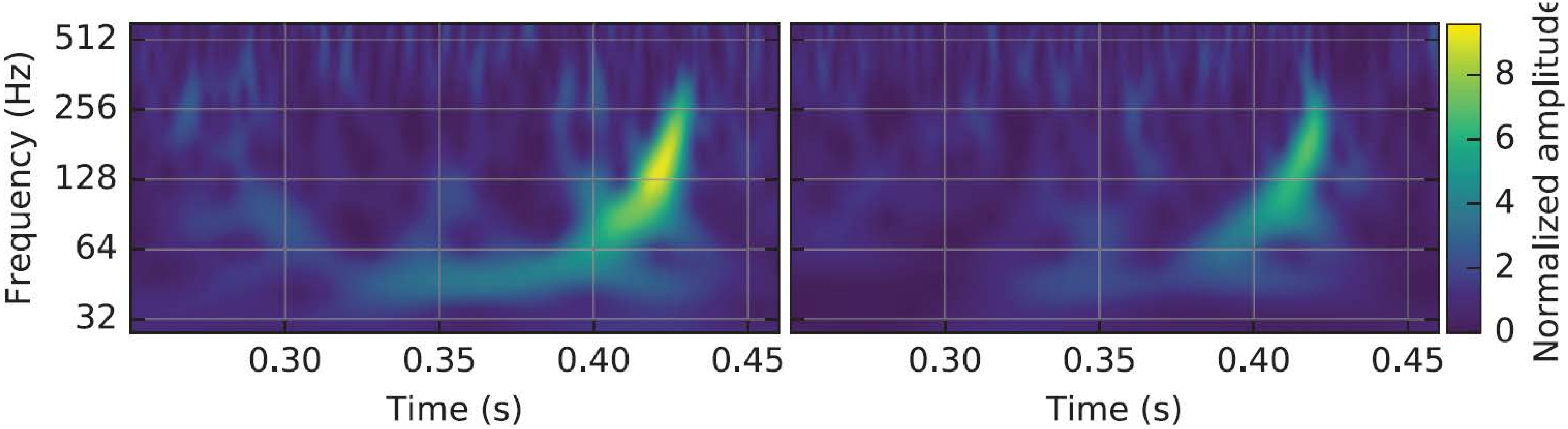

- ❑ Searching for GW signals, with a focus on
  - ➢ Compact binary coalescences
  - ➢ Ground-based detectors

From data to catalogs

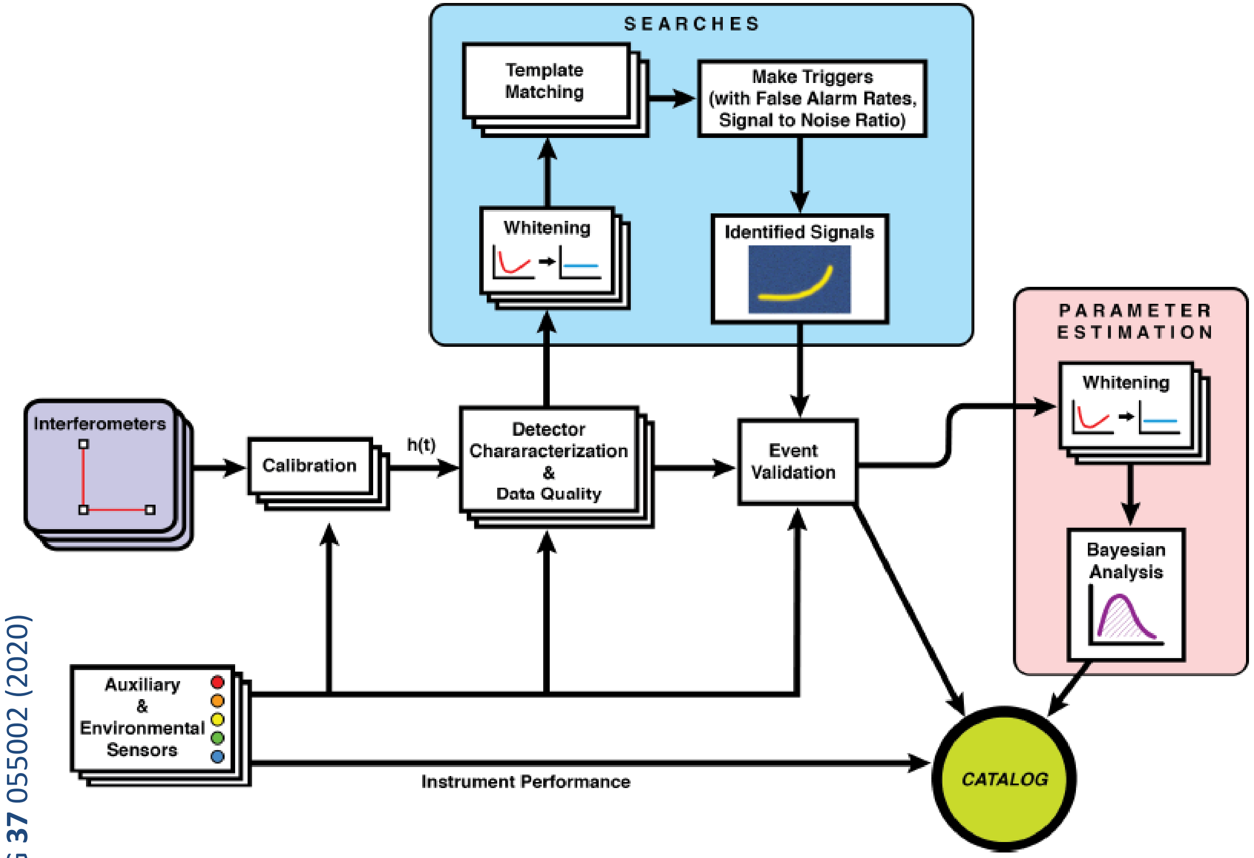

CQG **37** 055002 (2020)

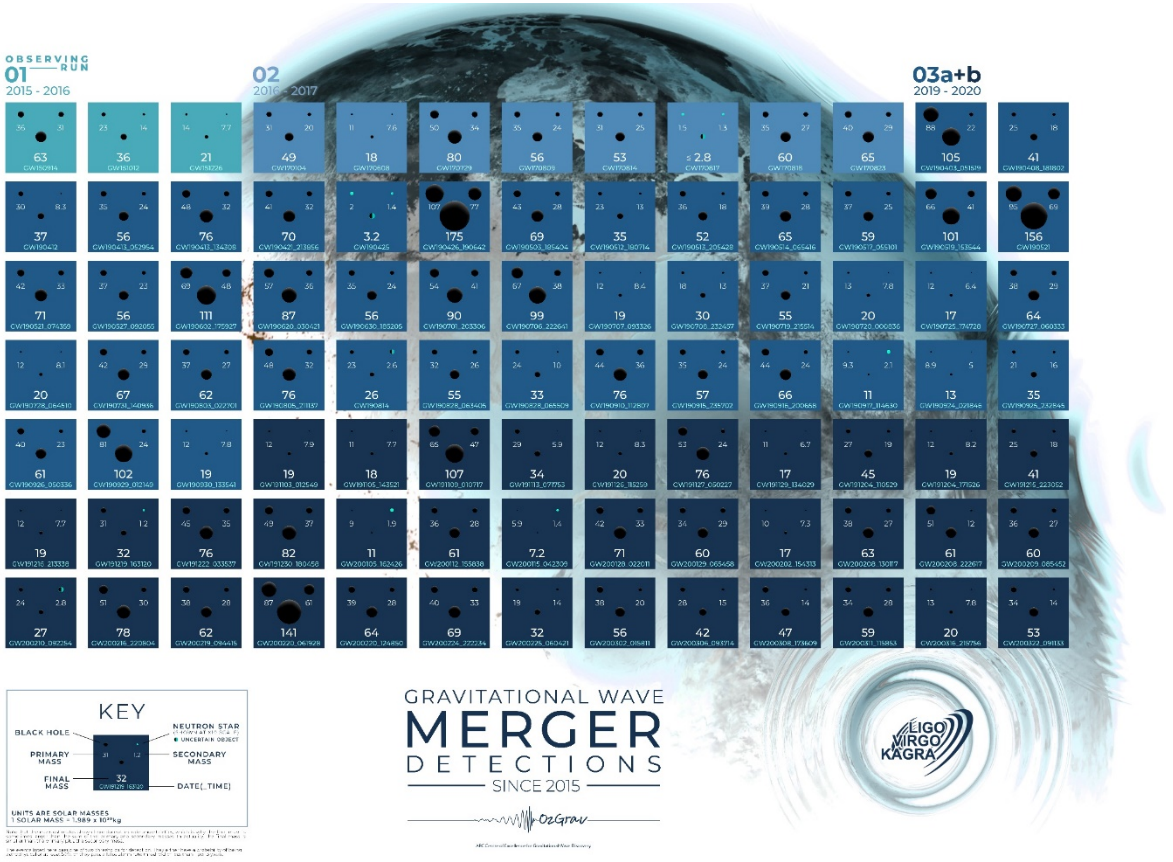

First things first: calibration

- Data analysis needs calibrated data
- Interferometer response calibrated against
  - Laser wavelength reference
  - Known mirror displacements from auxiliary laser radiation pressure, aka *photon calibrator (PCal)*
  - Known mirror displacements from gravitational coupling to nearby rotating masses, aka *Newtonian calibrator (NCal)*
- Detector is a maze of feedback loops
  - *h(t)* reconstruction needs to use control signals in addition to output power measurement
- Also need to check that timing is consistent across detectors
- Typical accuracy ~2-5% on amplitude, ~2-4 deg on phase
  - Has to get better to match the sensitivity progress
    - Especially for cosmology applications
- *h(t)* reconstruction typically includes some noise subtraction, aka *data cleaning*

Pipelines

- cWB — Generic search
- GstLAL
- MBTA
- PyCBC
- SPIIR

Dedicated searches

Run offline

Run online (low-latency)

The (inspiral) signal in a nutshell

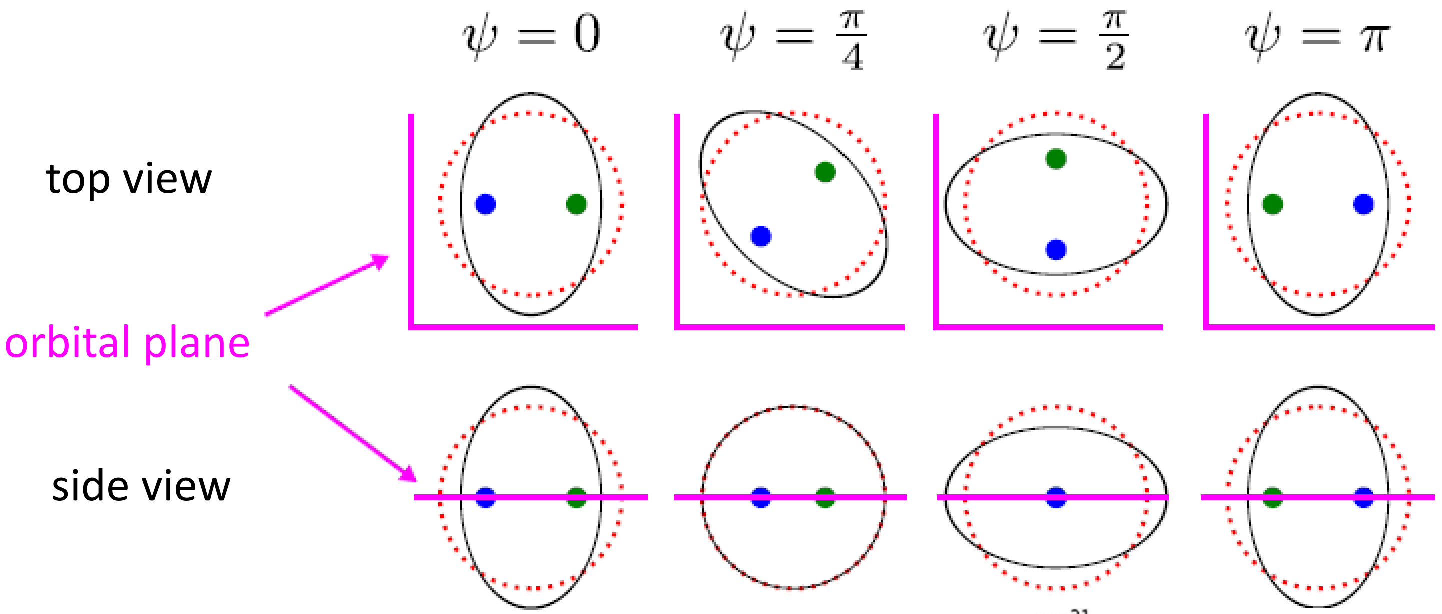

circular polarization

linear polarization

Dominant frequency

$$f_{\rm GW} = 2\ f_{\rm orbital}$$

Last stable orbit

$$f_{\rm ISCO} \sim \frac{3M_\odot}{M}\ 1500\ {\rm Hz}$$

$M(1+z)$ in practice

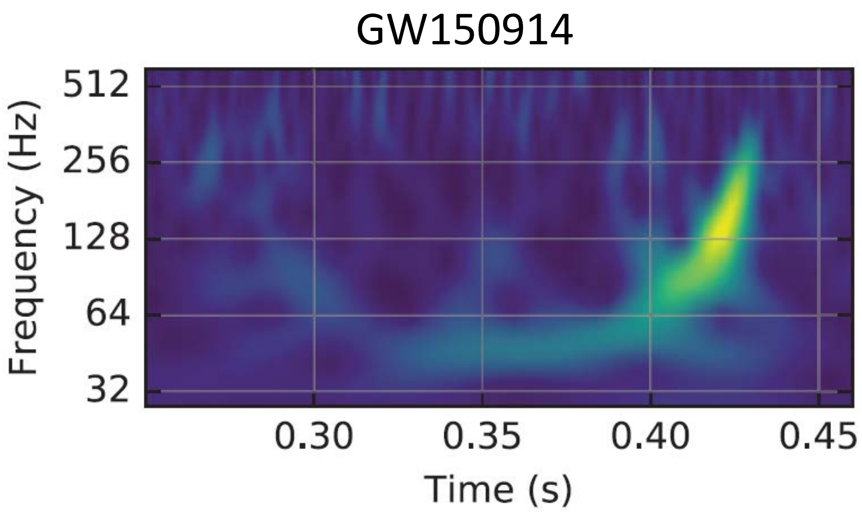

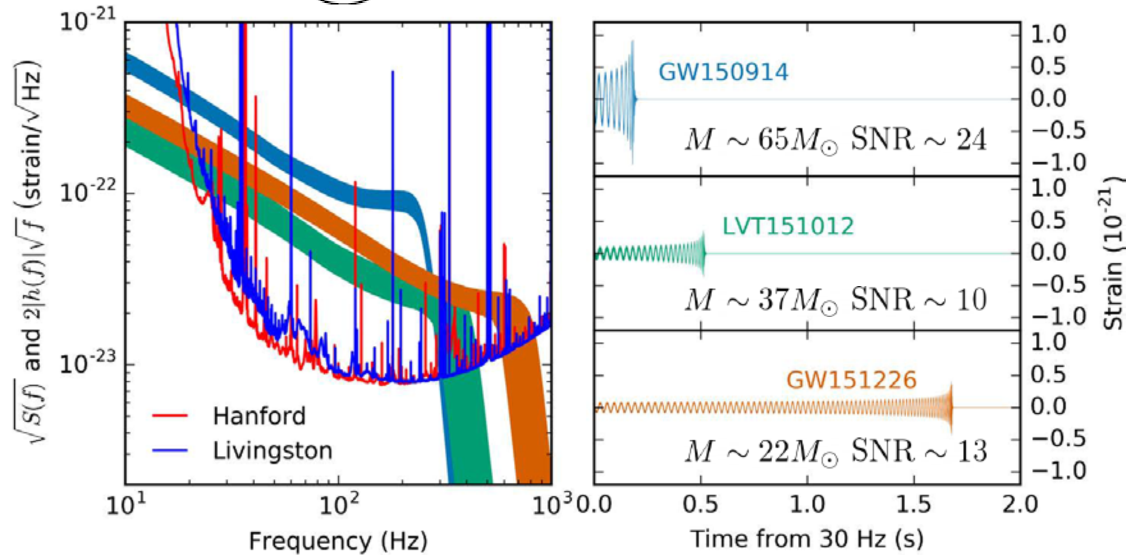

Matched filtering

$$S = (s|T) = 4\int_0^{\infty} \frac{\tilde{s}(f)\,\tilde{T}^*(f)}{S_n(f)}\,df$$

- If we know what we're looking for, and we know the properties of detector noise
- Correlation of data with expected signal, weighted by sensitivity curve

$$E[S] = \alpha \quad \text{if} \quad \tilde{s} = \alpha\,\tilde{T} + \tilde{n}$$
and T is properly normalized

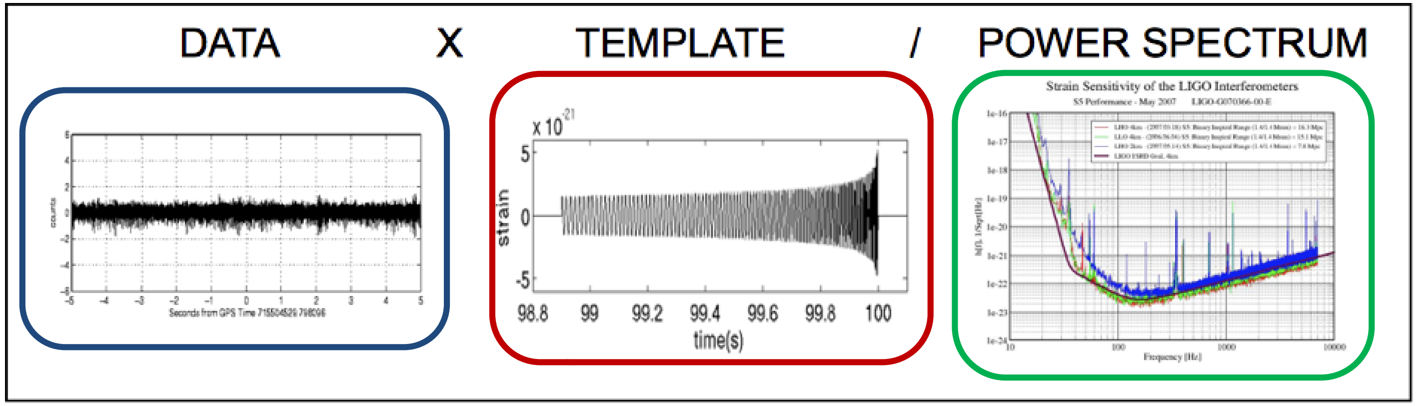

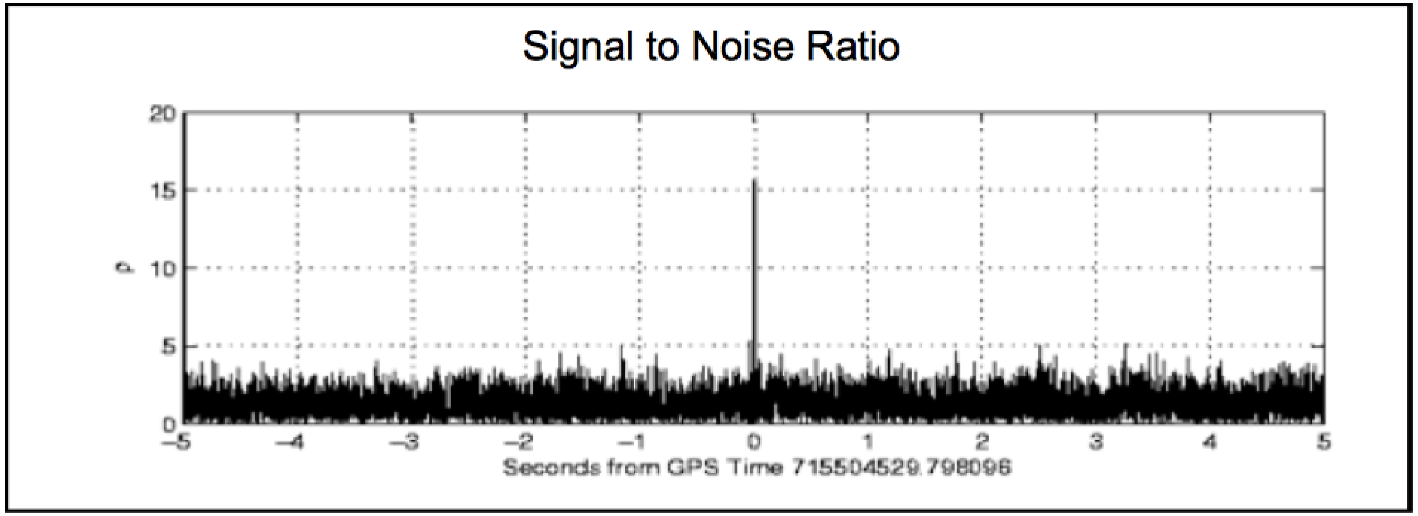

Matched filtering (cont.)

- As a function of the (unknown) arrival time

$$S(t_c) = 4\int_0^\infty \frac{\tilde{s}(f)\tilde{T}^*(f)}{S_n(f)} e^{-i2\pi f t_c} df$$

- Maximize over unknown phase

$$S(t_c) = 4\left|\int_0^\infty \frac{\tilde{s}(f)(\tilde{T}_{0^\circ}(f) - i\tilde{T}_{90^\circ}(f))^*}{S_n(f)} e^{-i2\pi f t_c} df\right|$$

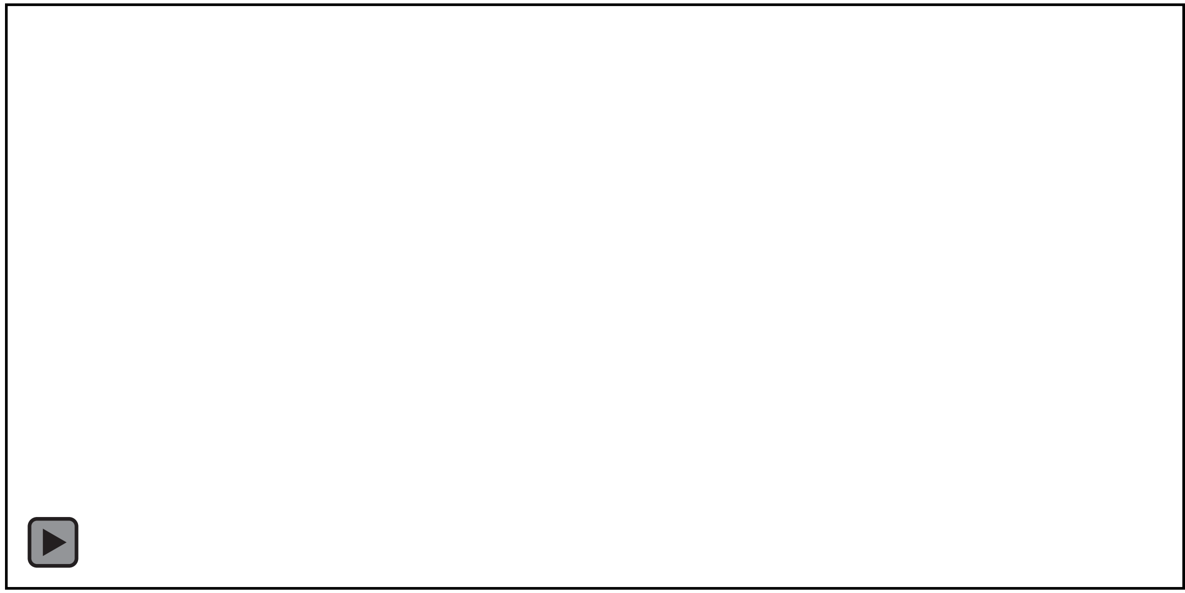

- Record *trigger* at t_c if $S(t_c)$ exceeds some threshold

Matched filtering is "optimal"

In Gaussian, stationary noise with known PSD…

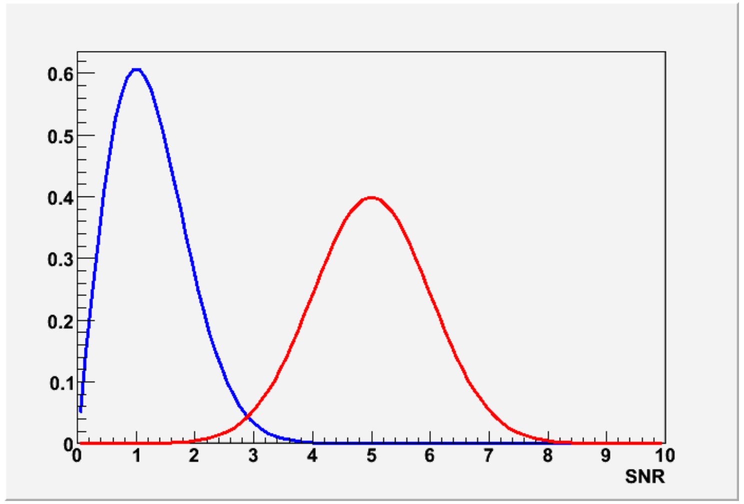

- Noise SNR distribution: χ^2 with 2 degrees of freedom
- Signal SNR distribution: non-central χ^2 distribution ~ Gaussian distribution if signal strong enough

- Matched filter optimizes SNR $\mathrm{SNR} = \frac{E[S]}{\sqrt{E[(S - E[S])^2]}}$

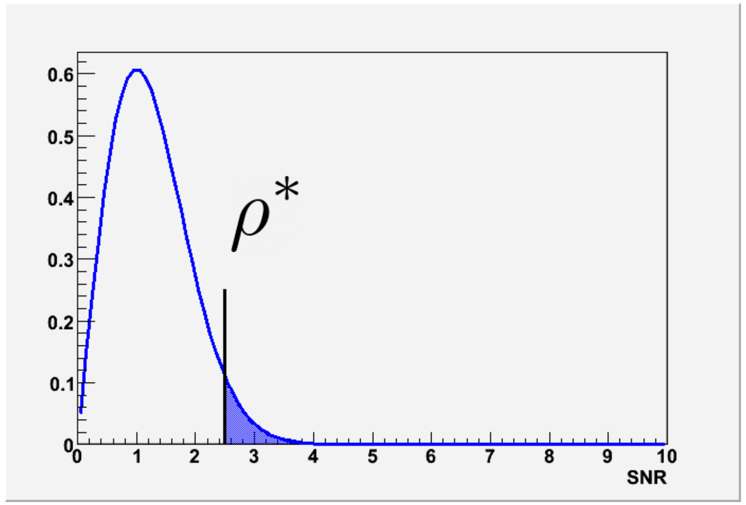

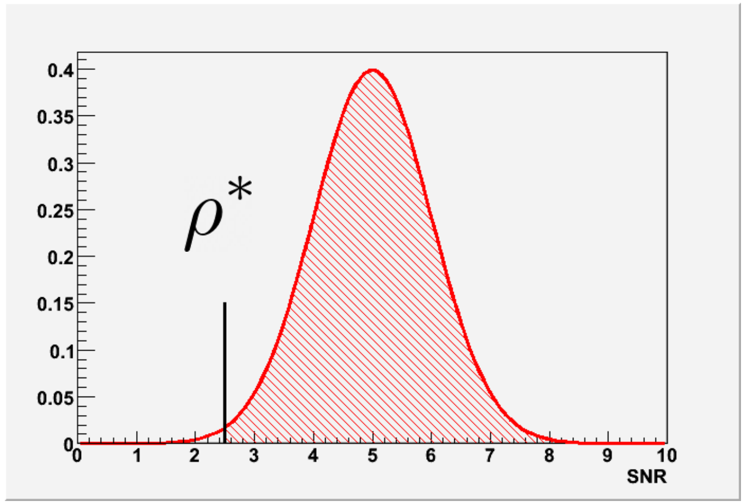

- Selecting triggers by setting threshold on SNR $\rho > \rho^*$ guarantees lowest false alarm probability for given detection probability

But…

Matched filtering SNR & likelihood ratio

- Likelihood ratio of signal vs noise

$$\Lambda = \frac{p(s|h)}{p(s|0)} = \frac{e^{-(s-h|s-h)/2}}{e^{-(s|s)/2}}$$

$$\ln \Lambda = (s|h) - \frac{1}{2}(h|h)$$

See part II of lecture for why the likelihood takes this form

- Take $h = \alpha h_0$ with $(\mathrm{h_0}|\mathrm{h_0}) = 1$

$$\ln \Lambda = \alpha(s|h_0) - \frac{\alpha^2}{2}$$

- Maximize $\ln \Lambda$

$$\frac{d \ln \Lambda}{d\alpha} = 0 \Rightarrow \alpha = (s|h_0)$$

$$\ln \Lambda_{\max} = \frac{1}{2}(s|h_0)^2 = \frac{1}{2}\rho^2$$

Noise spectrum

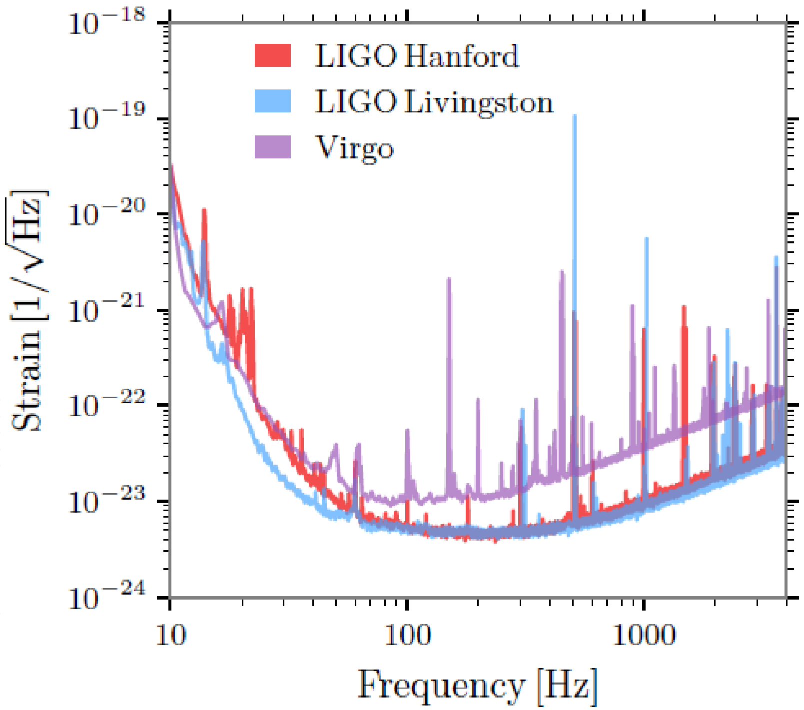

arXiv:2111.03606

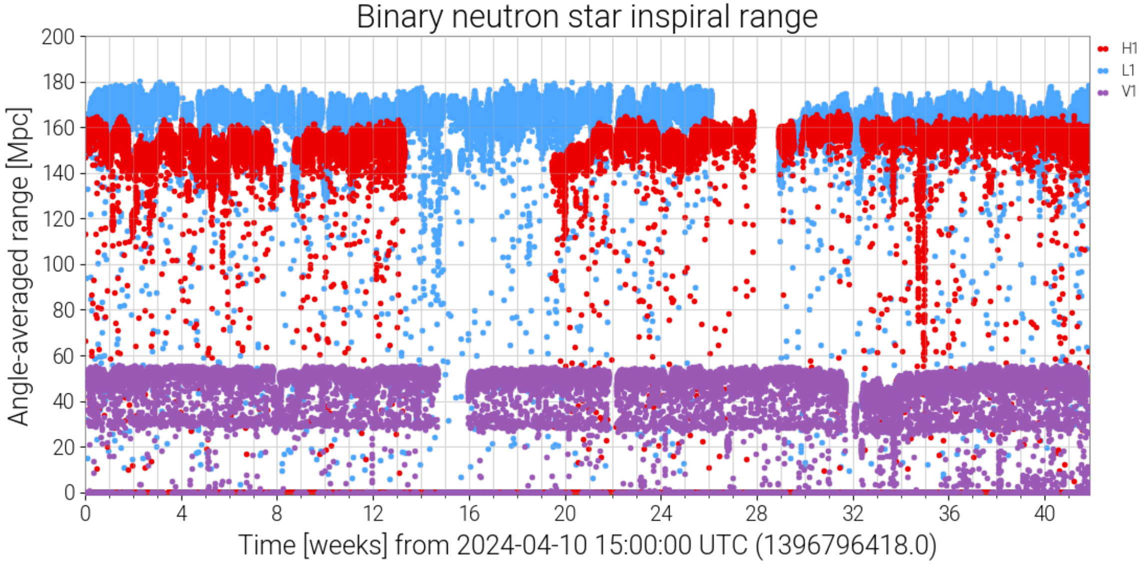

- ❑ Detector noise spectrum has complex structure
  - ➢ Broadband noise
  - ➢ Narrow features
  - ➢ Large dynamic range
- ❑ Noise spectrum is not stationary
- ❑ Estimated by averaging consecutive FFTs
  - ➢ Over time large enough to get smooth estimate, short enough to follow medium-term variations

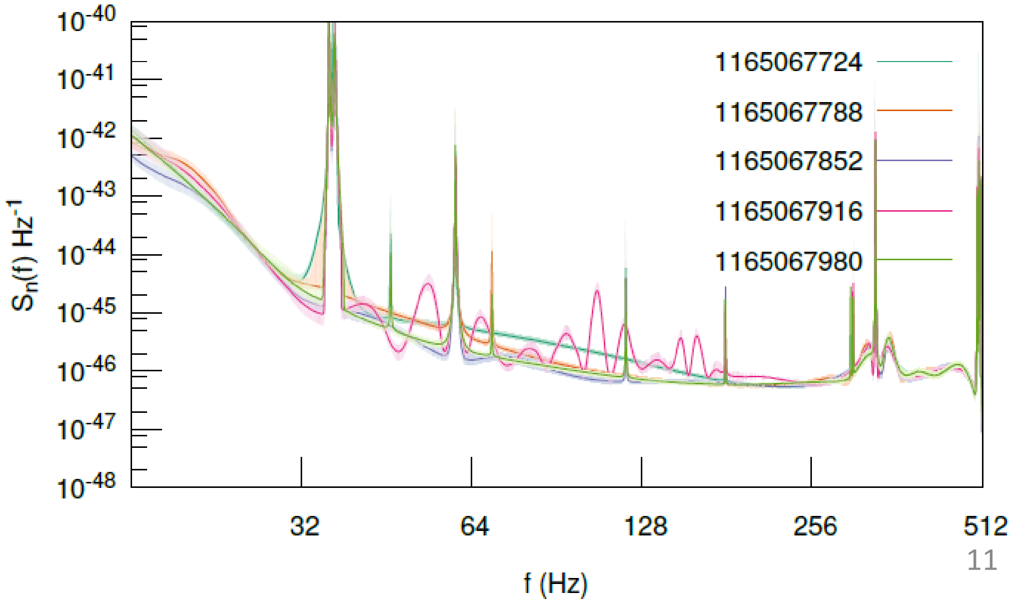

CQG 37 055002 (2020)

Waveforms

- Approximate analytical solutions
  - Perturbative approaches
    - Post-Newtonian expansion
    - Effective-one-body approach
    - Final black hole ringdown
  - Accurate for inspiral and ringdown, loses accuracy close to merger

- Numerical solutions
  - Solving Einstein's equations directly with numerical evolution methods
  - Computationally expensive
    - Cannot be used to model many orbits
  - Can model merger

- Hybrid models
  - Combining results from analytical and numerical approaches
  - Provide full inspiral-merger-ringdown waveforms

Signal model

- Received signal

$$h_+(t) - ih_\times(t) = \sum_{l\geq 2} \sum_{m=-l}^{l} \frac{h_{lm}(t,\boldsymbol{\lambda})}{D_\mathrm{L}} {}_{-2}Y_{lm}(\theta,\phi)$$

$$h_{lm}(t,\boldsymbol{\lambda}) = A_{lm}(t,\boldsymbol{\lambda}) e^{i\Phi_{lm}(t,\boldsymbol{\lambda})}$$

- Measured signal

$$h(t) = F_+(\Theta)h_+(t) + F_\times(\Theta)h_\times(t)$$

Parameters

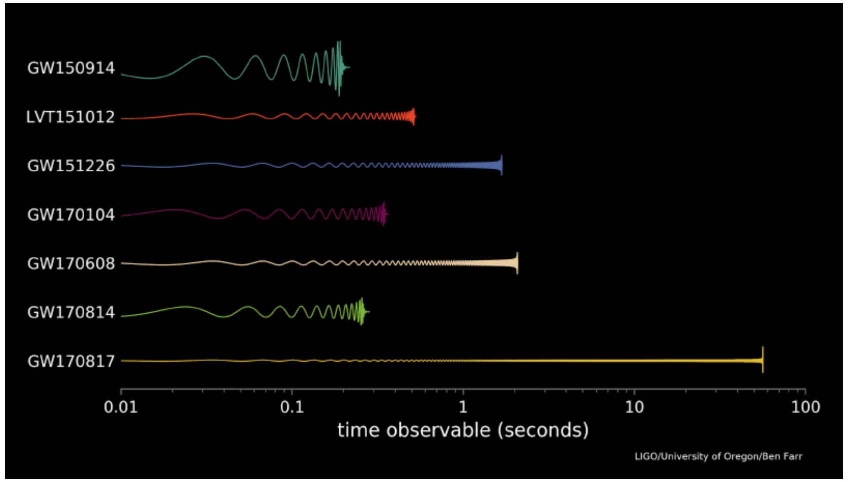

- In general, compact binary is described by up to 19 parameters
  - Intrinsic parameters drive system dynamics
    - Masses (2)
    - Spins (6)
    - Deformability for neutron stars (2)
    - Eccentricity (2)
  - Extrinsic parameters impact measured signal
    - Position : luminosity distance, right ascension, declination (3)
    - Orientation: inclination, polarization (2)
    - Time and phase at coalescence (2)

- Searching a reduced parameter space
  - Assume that there is no eccentricity
  - Assume that there is no precession of the orbital plane
  - Assume that both bodies are black holes
  - Restrict to the dominant mode of the signal $(l = 2)$
  - Orientation and location parameters now enter as overall scale, time or phase shifts, easily maximized over
  - Scan a 4-dimensional space: m_1, m_2, S_{1z}, S_{2z}

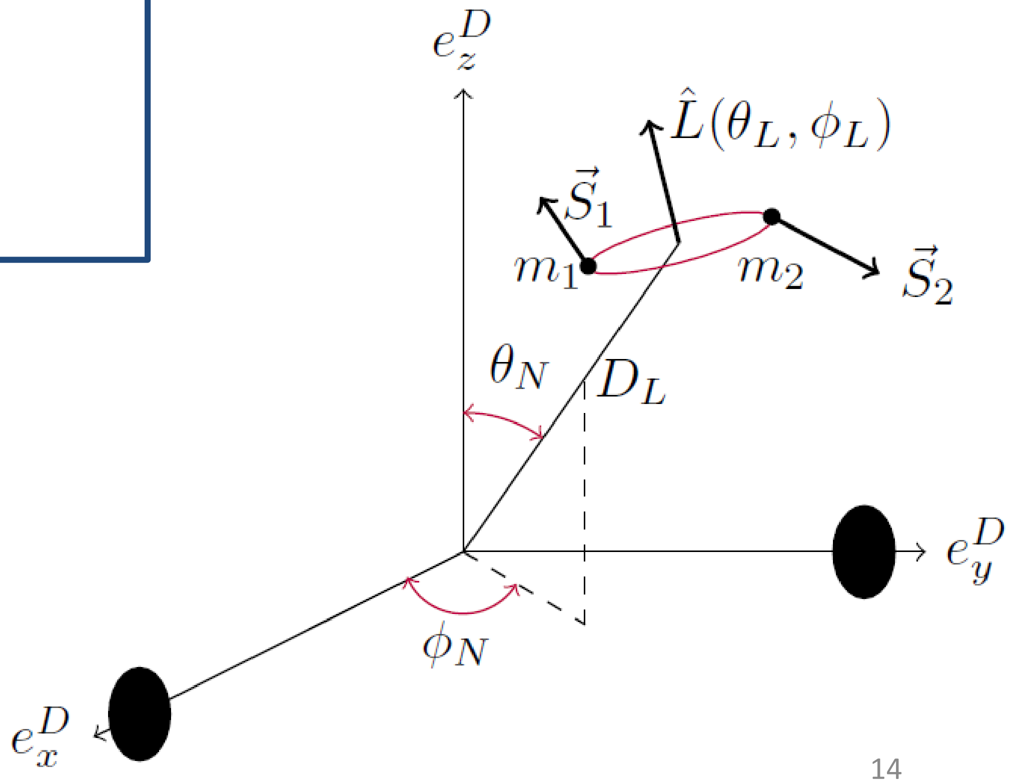

Template banks

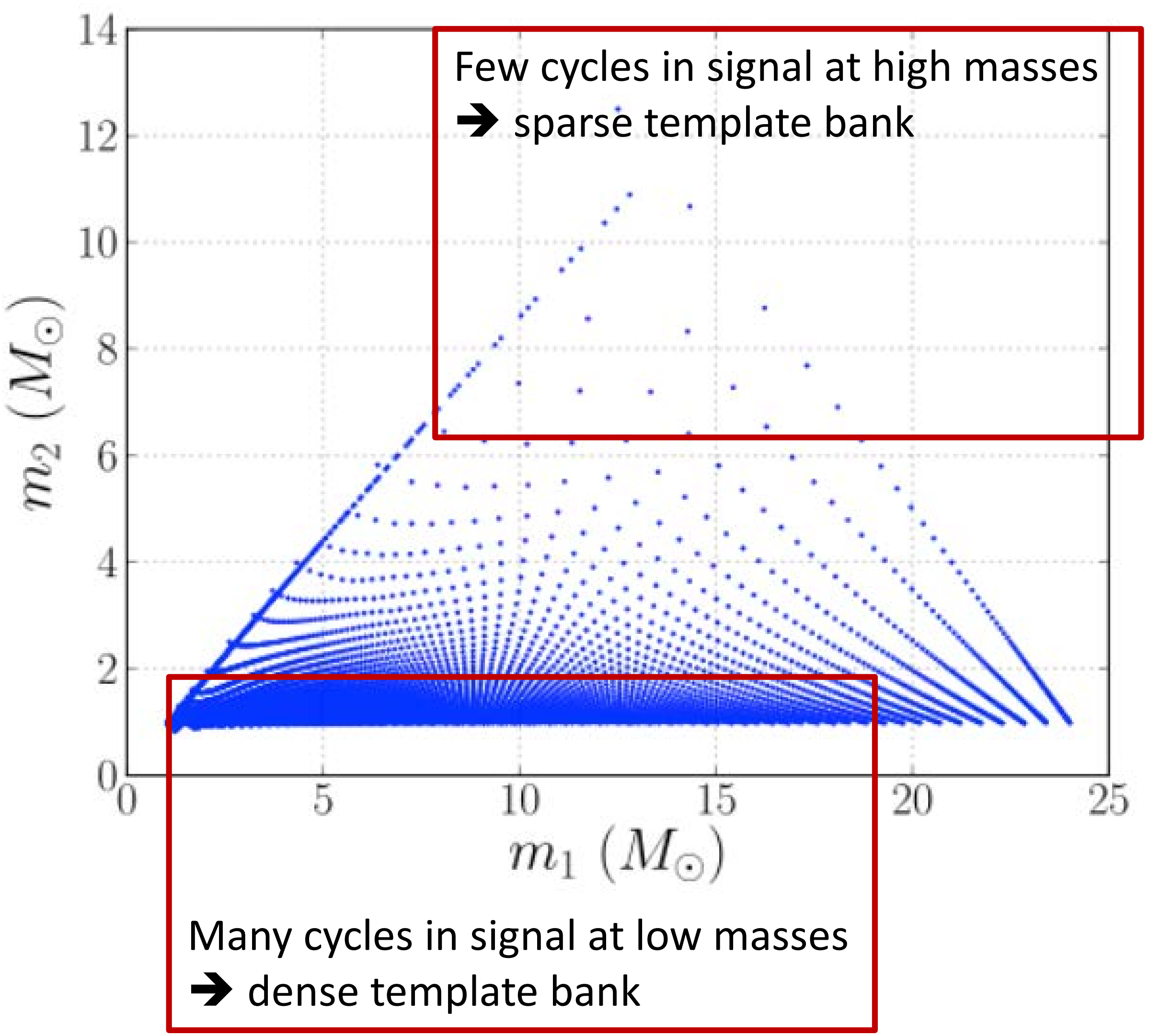

- Overlap (inner product)

$$(a|b) = 4\int_0^\infty \frac{\tilde{a}(f)\tilde{b}^*(f)}{S_n(f)}df$$

- Match

$$M(a,b) = \max_{t_c,\phi_c} \frac{(a|b)}{\sqrt{(a|a)}\sqrt{(b|b)}} \leq 1$$

- Fitting factor

$$\varphi = \max_i M(a, b(\boldsymbol{\theta}_i))$$

- Criterion for template bank

$$\varphi \geq \varphi_{\min}$$

  - Historically $\varphi_{\min} = 0.97$

- Optimize effectualness vs size

Building template banks

- Geometric placement
  - Quadratic approximation to the match

$$M(h(\boldsymbol{\theta}), h(\boldsymbol{\theta} + \delta\boldsymbol{\theta})) \sim 1 - g_{ij}\delta\theta_i\delta\theta_j$$

$$g_{ij}(\boldsymbol{\theta}) = \left.\frac{\partial M(h(\boldsymbol{\theta}), h(\boldsymbol{\lambda}))}{\partial\lambda_i\partial\lambda_j}\right|_{\boldsymbol{\lambda}=\boldsymbol{\theta}}$$

  - Reparametrize to a space where $g_{ij} \sim \text{constant}$
    - e.g. $(m_1, m_2) \rightarrow (\tau_0, \tau_3)$
  - Cover space with optimal grid (e.g. hexagonal in 2D)
  - Transform back to parameters that can be used to generate waveforms
- Very efficient
  - Metric cannot be easily computed for any waveform model

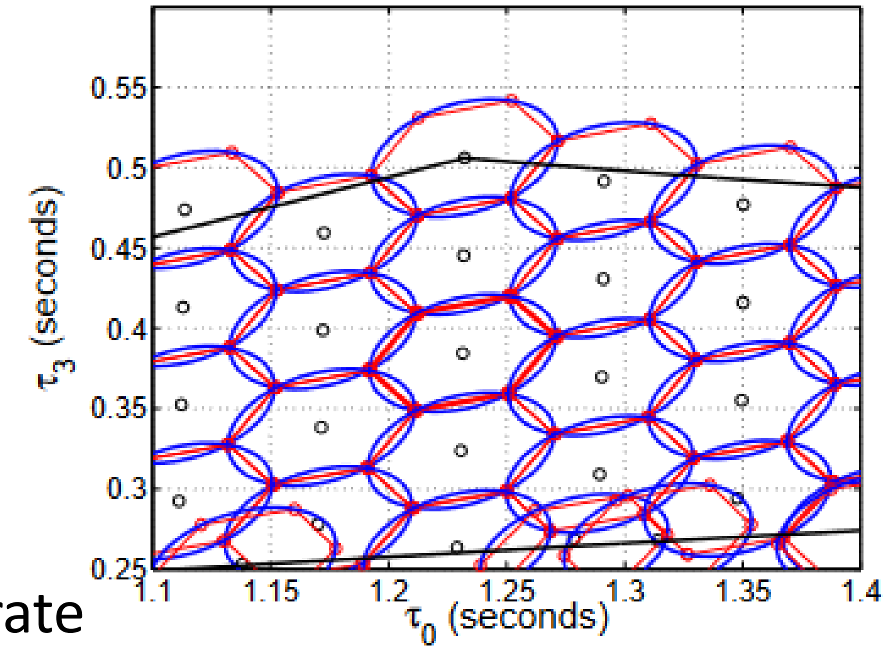

Chirp time at leading order

Building template banks (cont.)

- Stochastic placement
  - Pick a random point in the search space
  - Calculate the fitting factor with the previous points
  - If fitting factor smaller than 0.97, keep the new point
  - Iterate
- Straightforward and applicable with any waveform model
- Slow & does not guarantee complete coverage

- Hybrid banks
  - Searches typically use banks built upon a mix of geometric and stochastic placement

Template banks: example

- PyCBC O2 bank

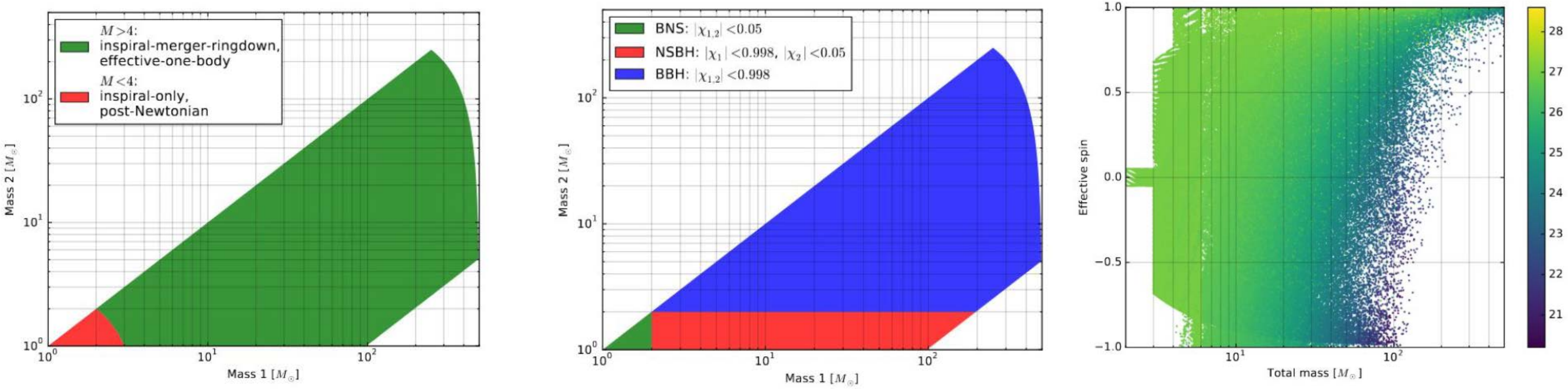

arXiv:1705.01845

Aligned spins extend the inspiral
Anti-aligned spins shorten the inspiral

Search parameter space

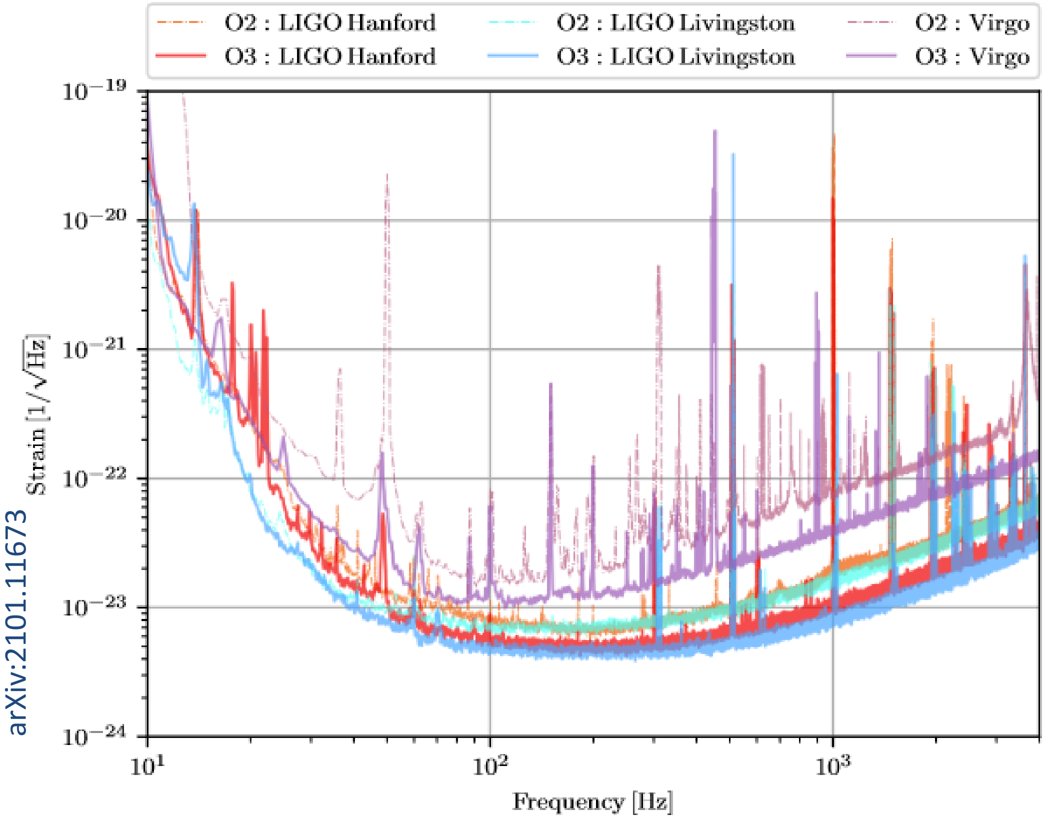

arXiv:2101.11673

- Detected masses are redshifted
  - For given (source-frame) parameter space, search parameter space needs to extend to higher masses as detector reach increases
- Number of observed cycles impacts density of template banks
  - For given parameter space, number of templates increases as low-frequency detector sensitivity improves and lower frequency cutoff decreases

- Main CBC search
  - $2 \leq M/M_\odot \leq\sim 500$
  - Template bank size ~ 4 10^5 (O2), ~ 8 10^5 (O3), 2 10^6 (O4)
- Sub-solar mass search
  - $0.2 \leq m_1/M_\odot \leq 10 \quad 0.2 \leq m_2/M_\odot \leq 1$
  - Template bank size ~ 1.9 10^6 $\quad f_{\rm low} = 45{\rm Hz}$
- Intermediate-mass BH search
  - $50 \leq M/M_\odot \leq 600$
  - Template bank size ~ 10^3

Noise is not Gaussian

- Environmental or instrumental artefacts are common in the data
  - Aka *glitches*
  - Responsible for long tails in SNR distributions
- Coping strategies
  - Use data quality tools to diagnose and flag issues where possible
  - Go beyond SNR by considering additional observables to distinguish between astrophysical signals and glitches
  - Estimate the background from the data
    - Requiring coincidence between detectors both reduces the background and provides ways to estimate it

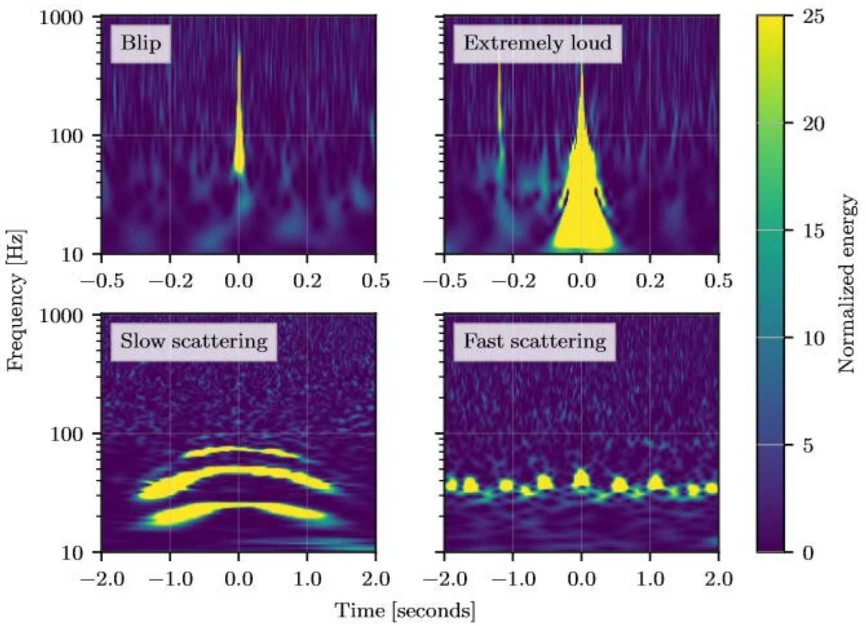

arXiv:2101.1167

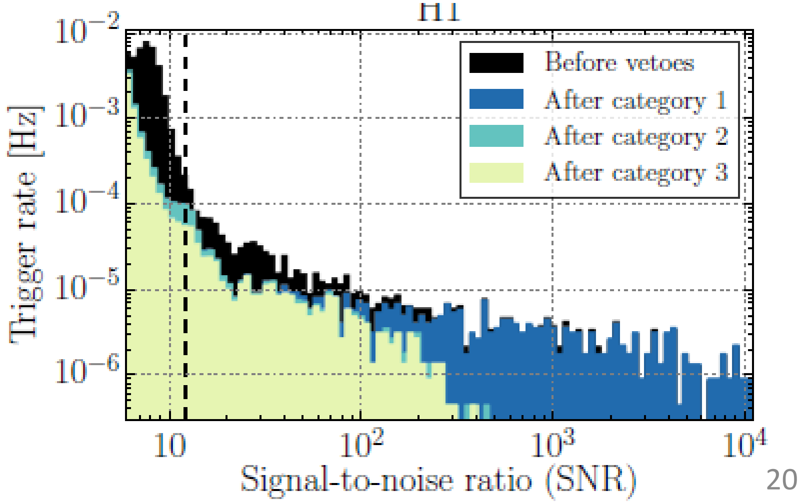

CQG 33 134001

Strategies to improve data quality

- Gating
  - Excise short stretches of data based on drops in instantaneous BNS range
    - Potentially unsafe but useful to use surrounding data and avoid biasing PSD

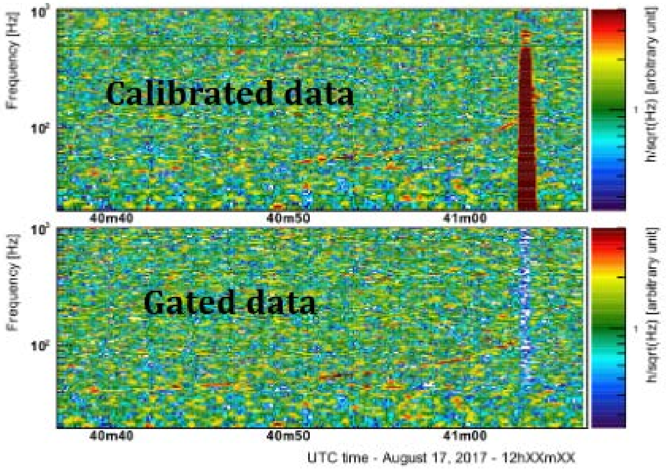

- Veto data or triggers based on data-quality flags
  - Using environmental and instrumental safe auxiliary channels

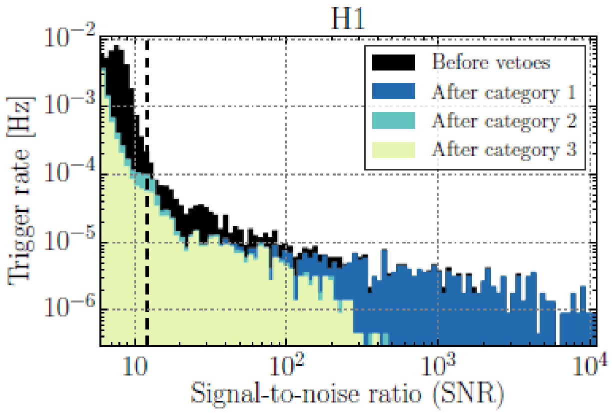

- iDQ
  - Supervised learning framework using safe auxiliary channels to predict glitch probability as a function of time

Signal consistency tests

- Is signal distributed over frequency band as expected?

$$\chi_r^2 = \frac{p}{2p-2}\sum_{i=1}^{p}\left(\rho_i - \frac{\rho}{p}\right)^2$$

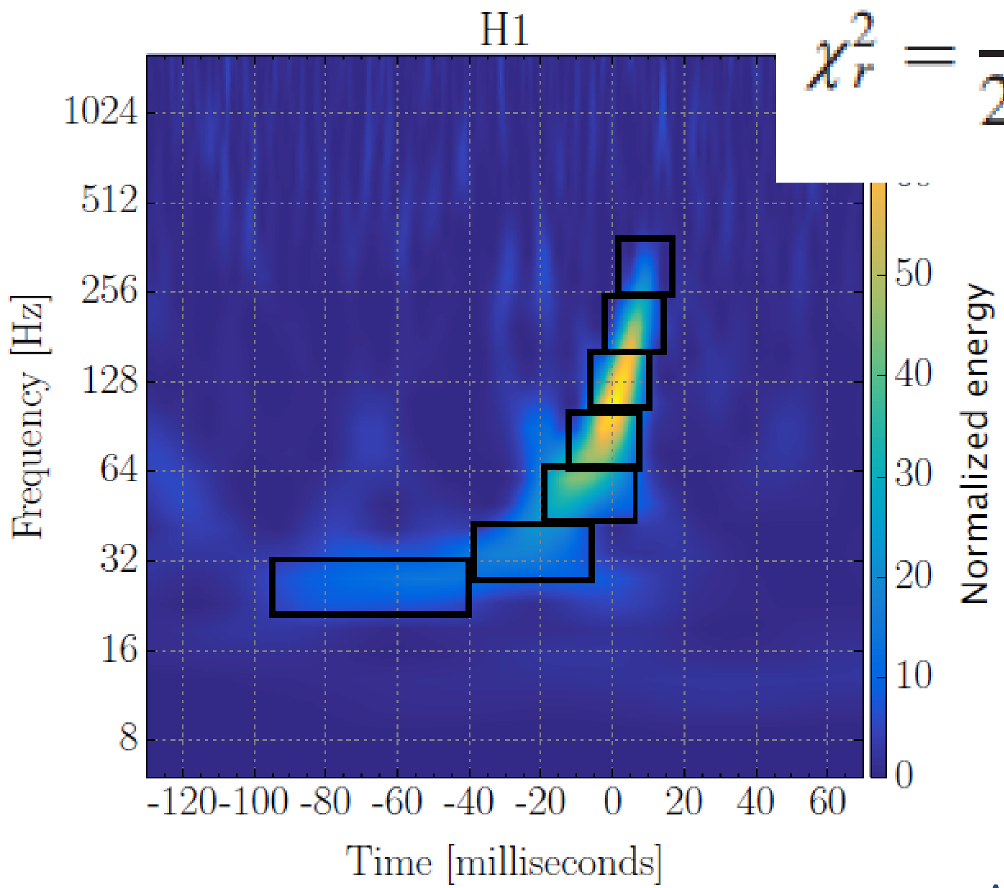

Astrophysical event

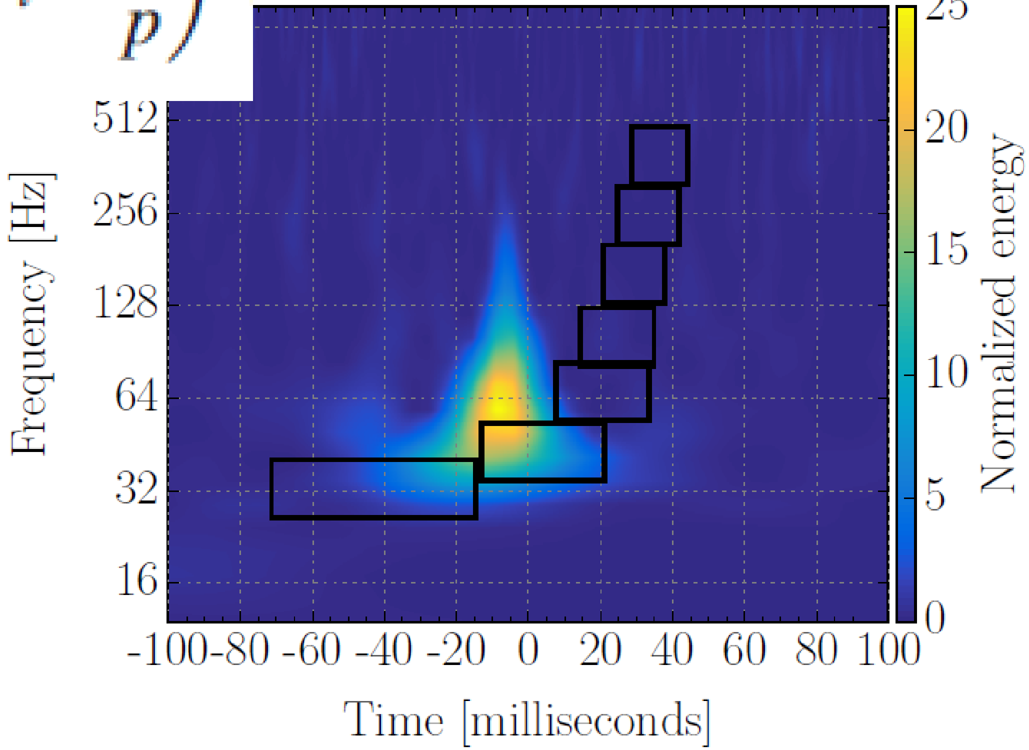

Instrumental artefact

Allen PRD 71 062001 (2005)

Signal consistency tests (cont.)

- Is SNR time series consistent with expected autocorrelation of template?

$$\xi^2_{\text{ac}} = \frac{1}{\mu} \int_{t_p+\delta t}^{t_p-\delta t} dt |\rho(t) - \rho_p R(t)|^2$$

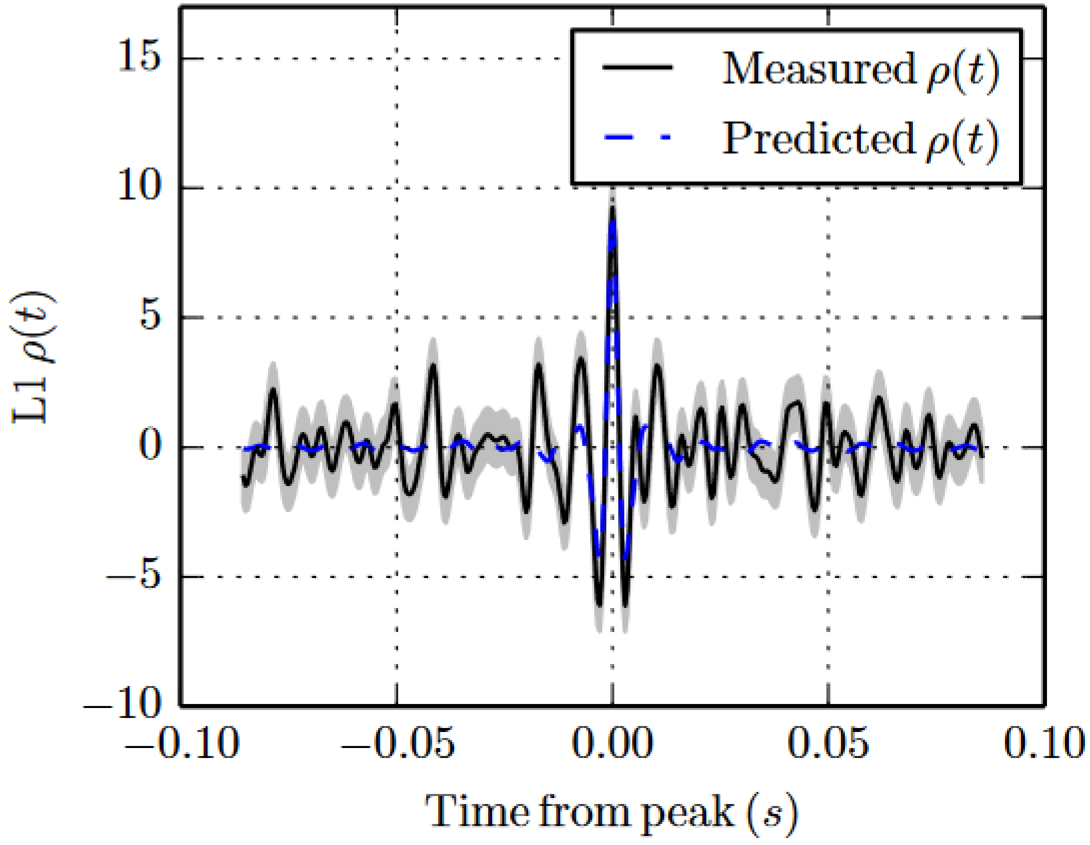

PRD 95, 042001 (2017)

Signal consistency across detectors

- Phase and time differences between detectors determined by source sky location and orientation with respect to detectors
  - Pattern expected for isotropic source population
  - Uniform distributions for noise
- Pattern also expected for SNR ratio between detectors, depending on detector sensitivities

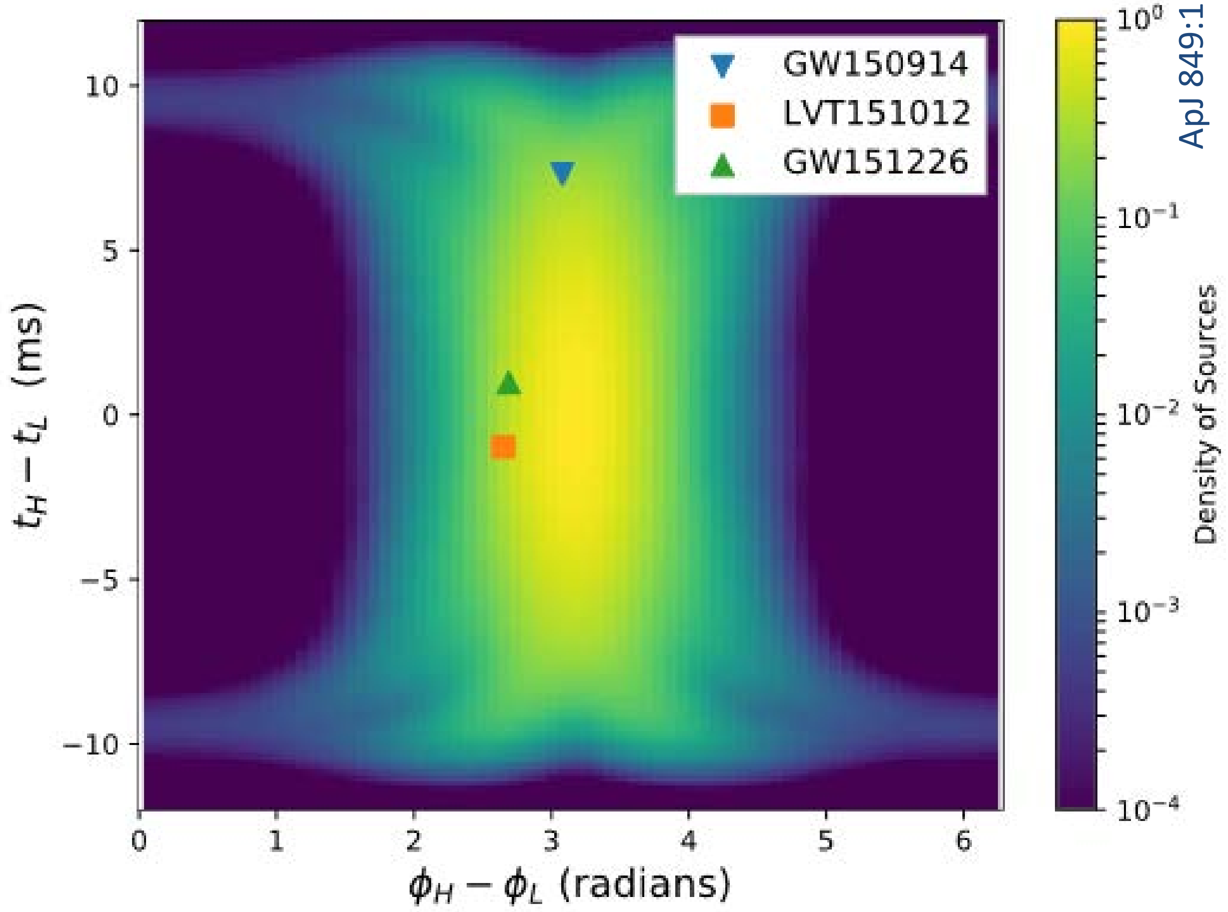

ApJ 849:118 (2017)

Ranking statistics

- Combine SNR with outcome of signal consistency tests to rank triggers

- PyCBC

$$\hat{\rho} = \begin{cases} \rho \Big/ [(1+(\chi_r^2)^3)/2]^{\frac{1}{6}}, & \text{if } \chi_r^2 > 1 \\ \rho, & \text{if } \chi_r^2 \le 1 \end{cases}$$

$$\hat{\rho}_c^2 = \hat{\rho}_{\mathrm{H}}^2 + \hat{\rho}_{\mathrm{L}}^2$$

$$\tilde{\rho}^2 = \hat{\rho}_c^2 + 2\log\left(\frac{p^S(\boldsymbol{\theta})}{p^S_{\max}}\right)$$

- GstLAL

$$\mathscr{L} = \frac{p(\mathbf{x}_{\mathrm{H}}, \mathbf{x}_{\mathrm{L}}, D_{\mathrm{H}}, D_{\mathrm{L}} | \theta_i, \mathrm{h})}{p(\mathbf{x}_{\mathrm{H}} | \theta_i, \mathrm{n})\, p(\mathbf{x}_{\mathrm{L}} | \theta_i, \mathrm{n})} \qquad \mathbf{x}_d = \{\rho_d, \xi_d^2\}$$

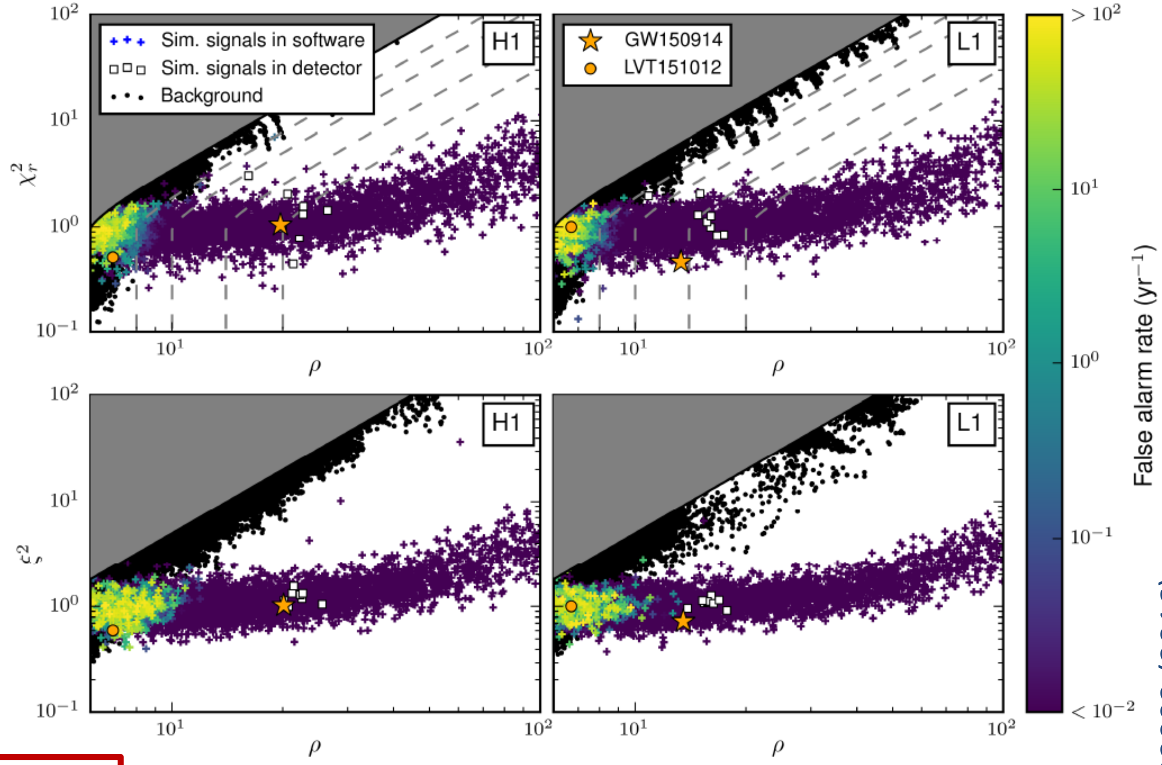

PRD 93, 122003 (2016)

Significance

- Coincidences
  - Triggers appearing in ≥ 2 detectors within coincidence time window, for the same template
- Construct a background from the data
  - Using some combination of single-detector triggers
- FAR: rate of noise events with same or higher ranking statistic value
- False alarm probability

$$\mathscr{F}(\hat{\rho}_c) \equiv P(\geq 1 \text{ noise event above } \hat{\rho}_c | T, T_b) = 1 - \exp\left[-T\frac{1 + n_b(\hat{\rho}_c)}{T_b}\right]$$

- Equivalent number of single-sided Gaussian standard deviations

$$-\sqrt{2}\,\mathrm{erf}^{-1}\left[1 - 2(1 - \mathscr{F})\right]$$

- Assigning a significance to single-detector triggers requires
  - Some extrapolation of FAR vs RS distribution
  - Being more aggressive at vetoing likely noise events
  - Being more conservative

Estimating the background

- ❑ With time slides

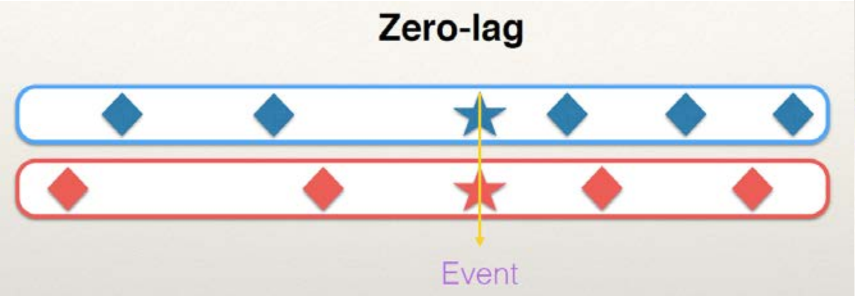

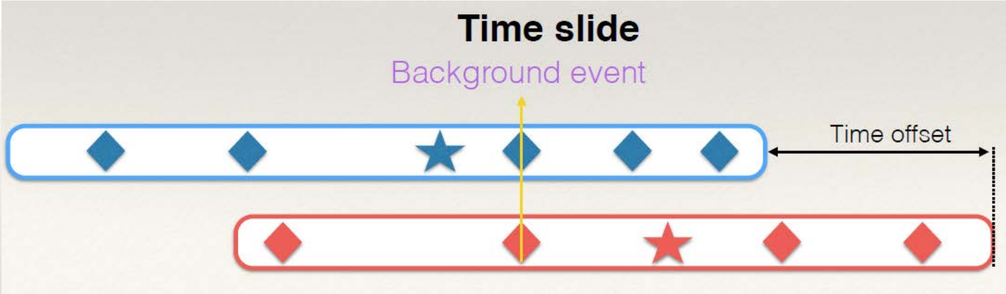

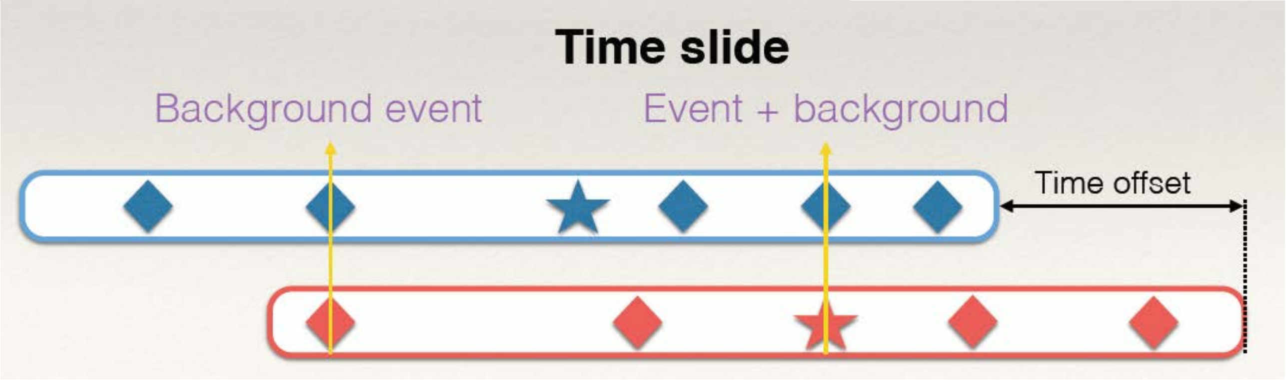

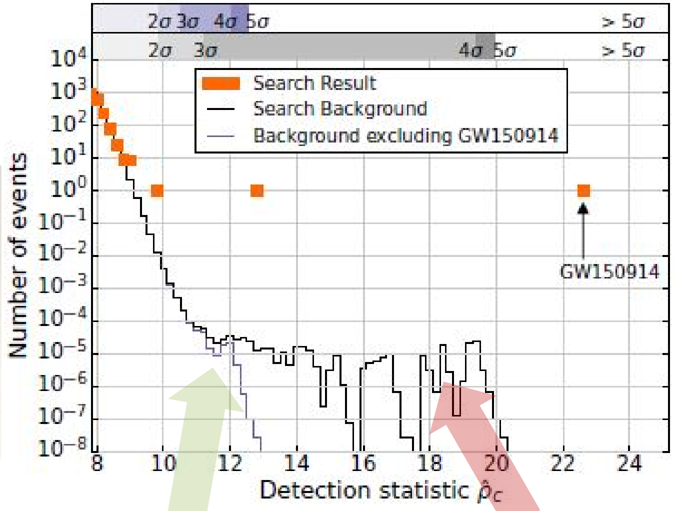

Hierarchical removal of confirmed signals from background to assess significance of other events

Coincidences between single detector triggers from GW150914 and noise in other detector

Background excluding contribution from GW150914 to gauge significance of other triggers

- ❑ Without time slides
  - ➢ Use all pairs of single-detector triggers
    - ▪ Account for probability that they could form a coincidence

IFAR plots

GWTC-1

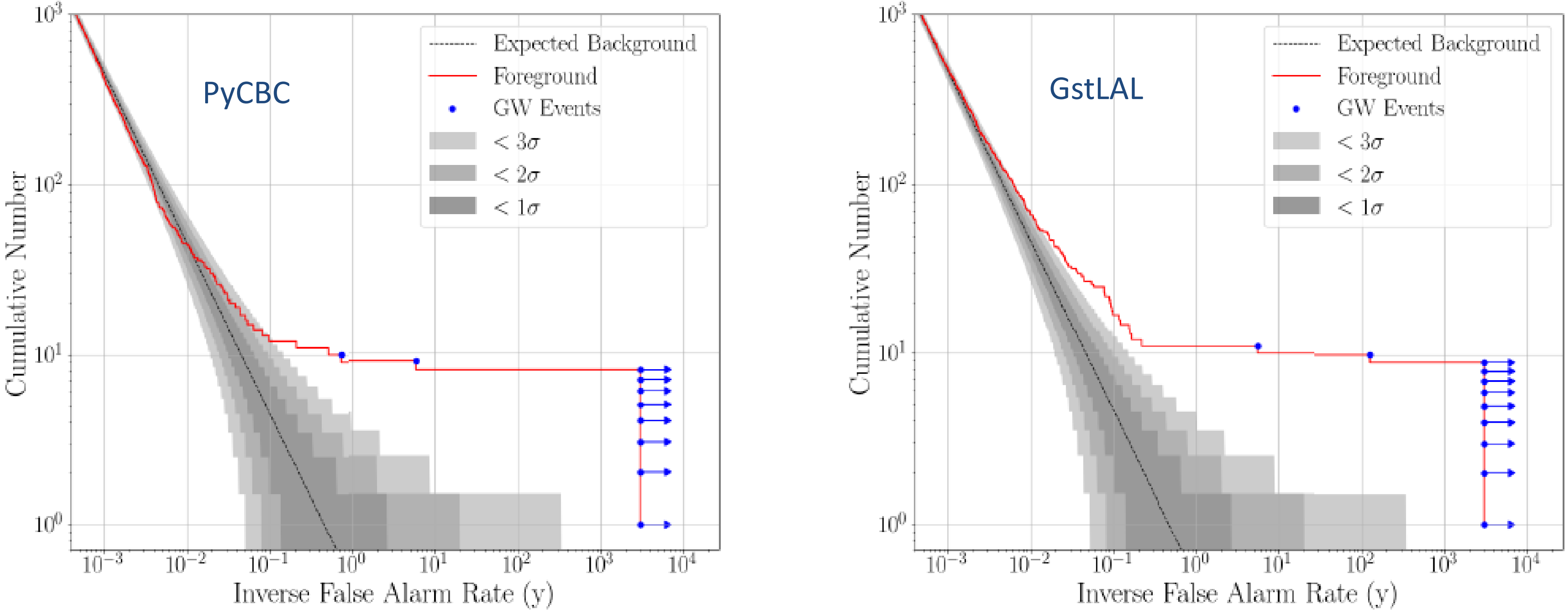

PRX 9, 031040 (2019)

IFAR plots (cont.)

- Cumulative number of triggers with IFAR ≥ x-axis value
- The expected background distribution is universal (modulo the analysis time)
  - O1+O2 analysis time T = 0.46 y
  - Expect on average 1 noise trigger with IFAR ≥ T, 2 with IFAR ≥ T/2, 3 with IFAR ≥ T/3, etc.
- The expected background distribution says nothing about the sensitivity of the search
  - The IFAR vs ranking statistic relationship does
  - If FARs reported by the search are self-consistent, noise triggers will follow the expected background distribution within statistical uncertainties
    - Number of noise triggers follows Poisson statistics
    - Error bars mark rates that can fluctuate up or down to *n* observed triggers at the 1, 2, 3 σ level, i.e. with probability

$$p = 0.3173/2\ (\pm 1\sigma)$$
$$p = 0.0455/2\ (\pm 2\sigma)$$
$$p = 0.0027/2\ (\pm 3\sigma)$$

  - Some systematic uncertainties too (non-stationarities)
- Foreground candidate events appear as outliers

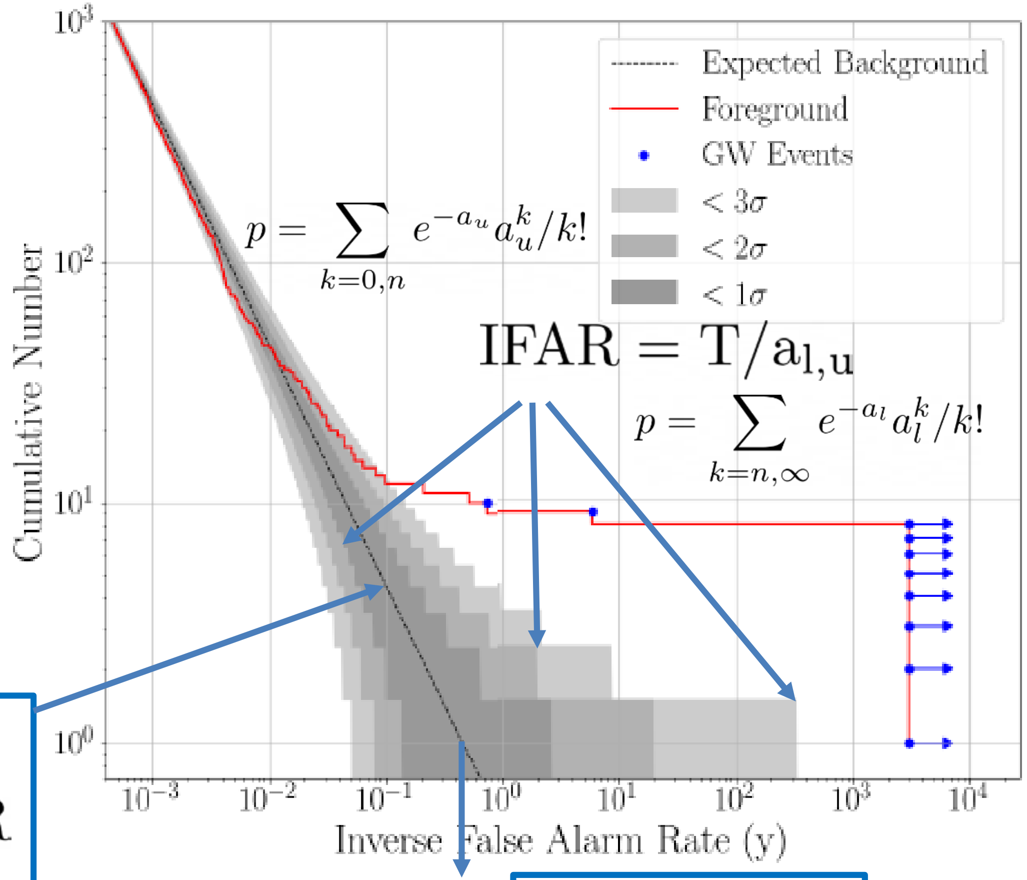

On average

$$n = T/\mathrm{IFAR}$$

T

One trigger per analysis time

Trials factors

- When assessing significance of candidate event coming from a template, wee need to take into account that:
  - We collect candidates from other templates
    - *Look-elsewhere effect*, aka *trials factor*
  - Search backgrounds are not uniform across templates
- Divide search space into classes (aka *bins*)
  - Background and local significance estimated within a given class
  - Global significance = local significance / number of classes

- Also account for different coincidence types, when data from 3 detectors are searched
  - HL, HV, LV, HLV

- GstLAL
  - 1 template = 1 bin
- MBTA
  - Several broad bins
- PyCBC
  - 1 bin
  - Ranking statistic modified to account for actual background distribution in each template ➔ ranking statistic distribution more uniform across templates

$$p^N \sim e^{-(\rho_{\mathrm{H}}^2+\rho_{\mathrm{L}}^2)/2}$$

$$\rightarrow \; p^N(\boldsymbol{\theta}) \propto \lambda_H^N(\hat{\rho}_H, \tau)\lambda_L^N(\hat{\rho}_L, \tau)$$

ApJ 849:118 (7pp), 2017

Burst generic search method

- Robust search paradigm
  - Require coherent signals in multiple detectors, using direction-dependent antenna response
  - Look for excess power in time-frequency space
    - Using wavelet decomposition
- Detection statistic
  - E_c dimensionless coherent signal energy obtained by cross-correlating the two reconstructed waveforms
  - E_n dimensionless residual noise energy after reconstructed signal is subtracted from data

$$\eta_c = \sqrt{\frac{2E_c}{(1 + E_n/E_c)}}$$

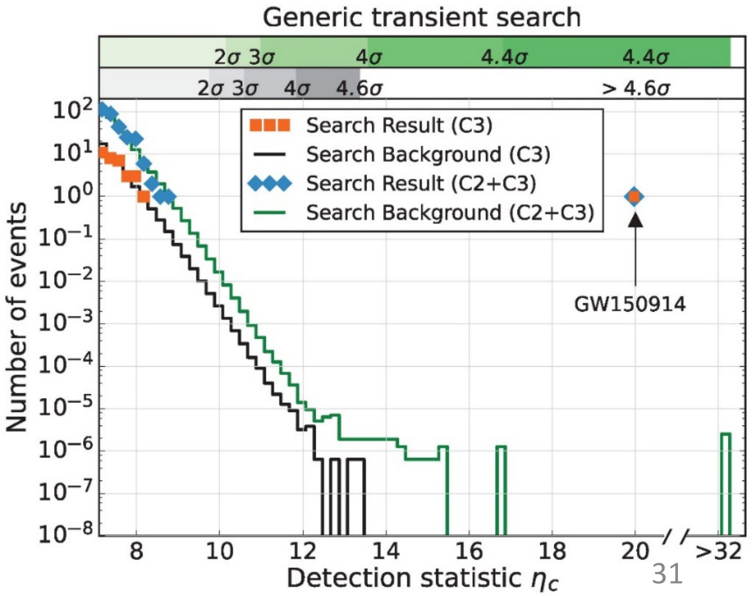

PRL 116, 061102 (2016)

- Getting the background under control is a challenge
  - No waveform assumed
    - But class for signal morphologies consistent with chirp
  - Noise artifacts have greater impact than for CBC searches, especially at lower frequencies

  ➔ Data quality and vetoes

Injections and search sensitivity

- Simulated signals added to data in software, aka *injections*
  - Used to design and tune signal consistency tests
  - Used to validate analysis
  - Used to estimate search sensitivity

$$\langle VT\rangle_{\{\theta\}} = T_{\mathrm{obs}} \int_0^\infty f(z|\{\theta\}) \frac{dV}{dz} \frac{1}{1+z} dz$$

$$\hat{N} = \langle VT\rangle R$$

Source population characteristics

Detection efficiency

Expected number of detections

Merger rate per unit volume and unit observing time

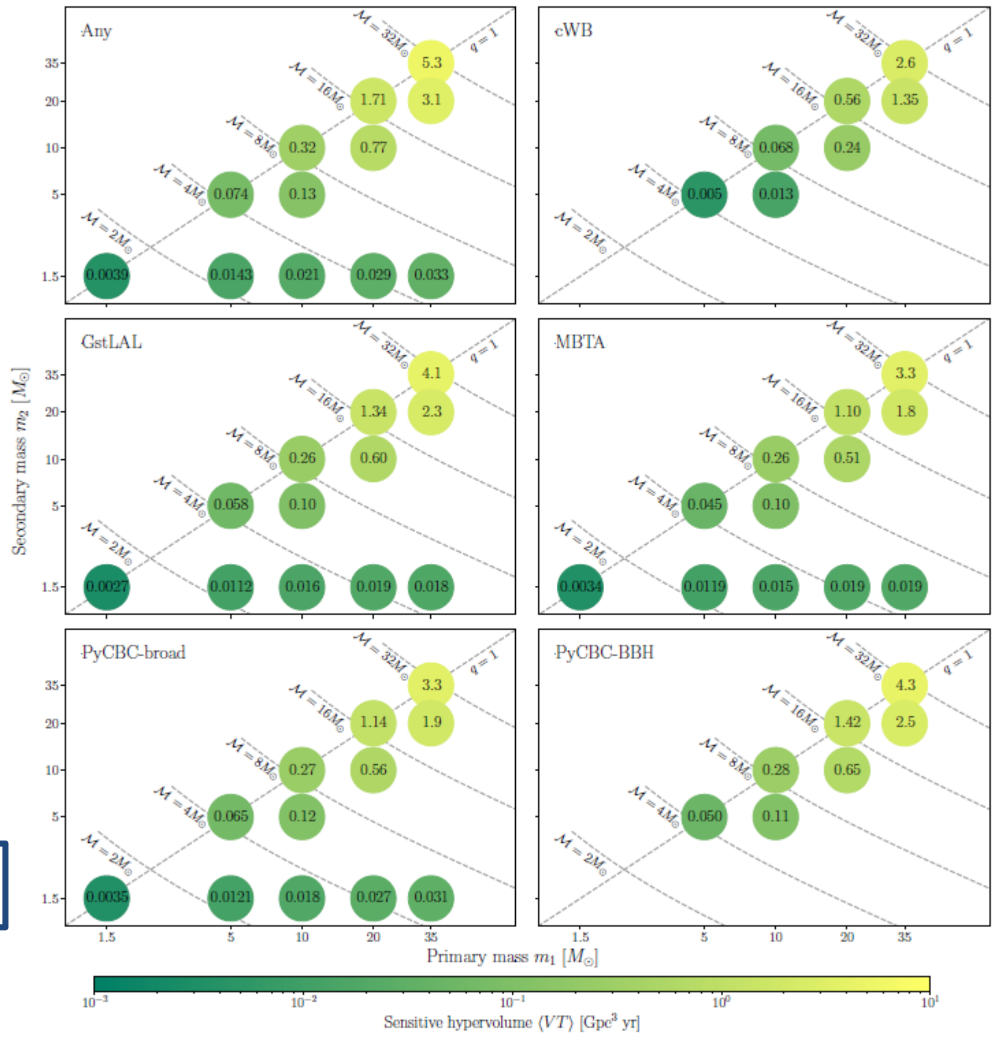

arXiv:2111.03606

Probability of astrophysical origin

$$p_{astro} = \frac{\text{foreground}}{\text{background} + \text{foreground}} = \frac{\Lambda_1 f(x)}{\Lambda_0 b(x) + \Lambda_1 f(x)}$$

Expected number of foreground events

Astrophysical foreground density
Estimated by projecting population model onto data

Expected number of background events

Background density
Estimated from data

Farr et al. PRD 91 023005 (2015)

Kapadia et al. CQG 37 045007 (2020)

$$\vec{\Lambda}_1 = \{\Lambda_{BNS}, \Lambda_{NSBH}, \Lambda_{BBH}\} \qquad \vec{f} = \{f_{BNS}, f_{NSBH}, f_{BBH}\}$$

$$p_\alpha(x|\vec{x}) = \int_0^\infty p(\Lambda_0, \vec{\Lambda}_1|\vec{x}) \frac{\Lambda_\alpha f_\alpha(x)}{\Lambda_0 b(x) + \vec{\Lambda}_1 . \vec{f}(x)} \mathrm{d}\Lambda_0 \, \mathrm{d}\vec{\Lambda}_1 \quad \Rightarrow p_{astro}(x|\vec{x}) = \sum_\alpha p_\alpha(x|\vec{x})$$

Name	Inst.	cWB			GstLAL			MBTA			PyCBC-broad			PyCBC-BBH		
		FAR (yr^{-1})	SNR	p_{astro}	FAR (yr^{-1})	SNR	p_{astro}	FAR (yr^{-1})	SNR	p_{astro}	FAR (yr^{-1})	SNR	p_{astro}	FAR (yr^{-1})	SNR	p_{astro}
GW191103_012549	HL	–	–	–	–	–	–	*27*	*9.0*	*0.13*	4.8	9.3	0.77	0.46	9.3	0.94
GW191105_143521	HLV	–	–	–	*24*	*10.0*	*0.07*	0.14	10.7	>0.99	0.012	9.8	>0.99	0.036	9.8	>0.99
GW191109_010717	HL	<0.0011	15.6	>0.99	0.0010	15.8	>0.99	1.8×10^{-4}	15.2	>0.99	0.096	13.2	>0.99	0.047	14.4	>0.99
GW191113_071753	HLV	–	–	–	–	–	–	26	9.2	0.68	*1.1×10^{4}*	*8.3*	*<0.01*	*1.2×10^{3}*	*8.5*	*<0.01*

arXiv:2111.03606

Offline vs online analyses

- Online analyses
  - Are configured to minimize latency
  - Use online calibrated data
  - Have access to limited data quality information
  - Can only assess data based on past information
  - Have a limited set of background events
  - Use FAR threshold to send alerts

- Offline analyses
  - Use data with final calibration and cleaning
  - Have access to final data quality information
  - Analyze data in *chunks* representing ~ 1 week of coincident data
  - Assess significance with respect to background in chunk / full run
  - Use *p_astro* threshold for inclusion in catalogs

Early warning

- At design sensitivity of advanced detectors
  - ~ 49% of detectable BNS detected 10 s before merger
  - ~ 7% 60 s before merger
  - ~ 2% detected before merger with localization ≤ 100 deg^2

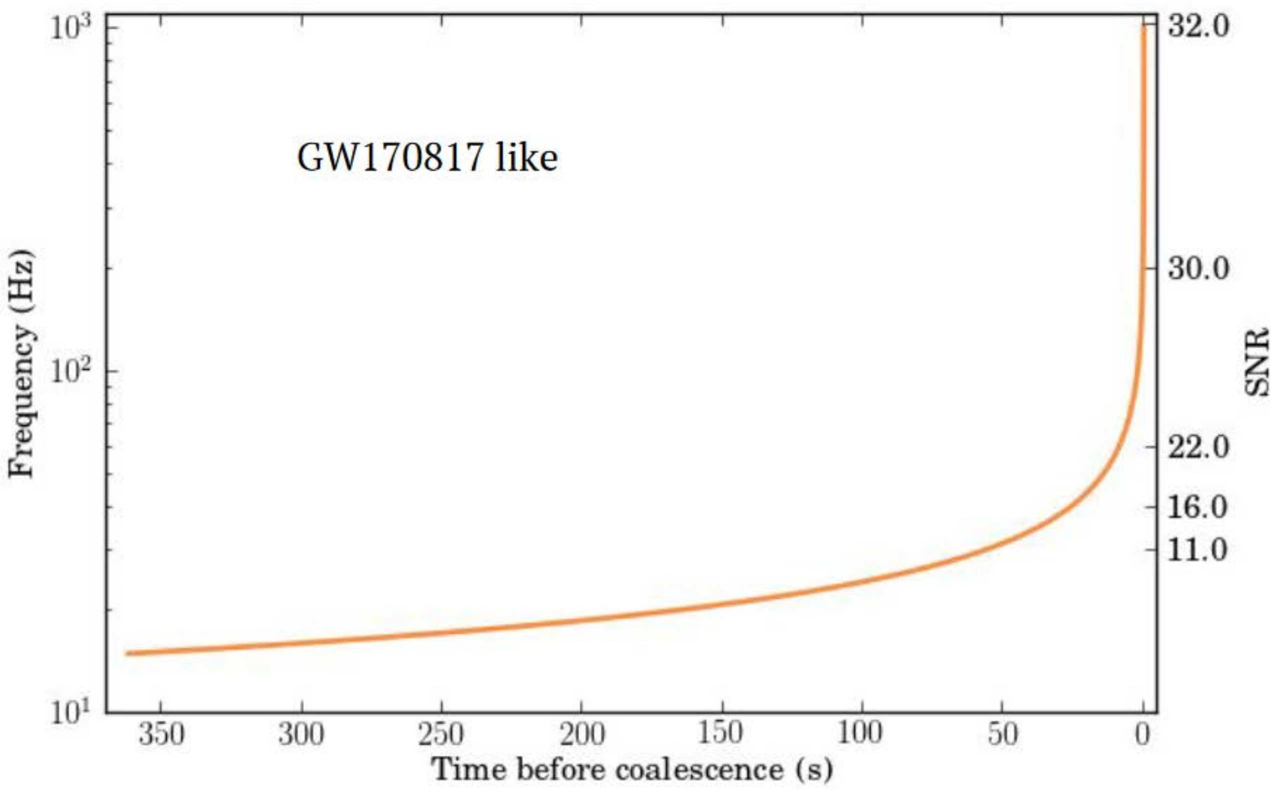

f_{high} (Hz)	$\langle VT \rangle$(Gpc^3 a)	$N_{signals}$(a^{-1})	$N_{low} - N_{high}$(a^{-1})
29	2.55×10^{-4}	3.21	0.775 – 8.71
32	3.84×10^{-4}	4.84	1.17 – 13.2
38	7.23×10^{-4}	9.12	2.20 – 24.8
49	1.45×10^{-3}	18.2	4.41 – 49.5
56	1.88×10^{-3}	23.6	5.71 – 64.2
1024	3.86×10^{-3}	48.7	11.8 – 132

arXiv:2008.04288

GRB triggered searches

- GRB & GW
  - Long GRBs are extreme cases of stellar collapse
  - BNS or NSBH mergers progenitors or short, hard GRBs
- Search data around times of GRBs observed by γ - Xray satellite based instruments
  - O1-O2-O3: > 300 GRBs with enough data to be analyzed
    - 1 coincident detection GW170817
  - Short GRBs analyzed with BNS and NSBH search, short & long GRBs analyzed with burst search
- Triggered searches
  - Small amount of data searched leads to lower background and better sensitivity
  - Known sky position makes coherent search across detectors possible also for CBC search

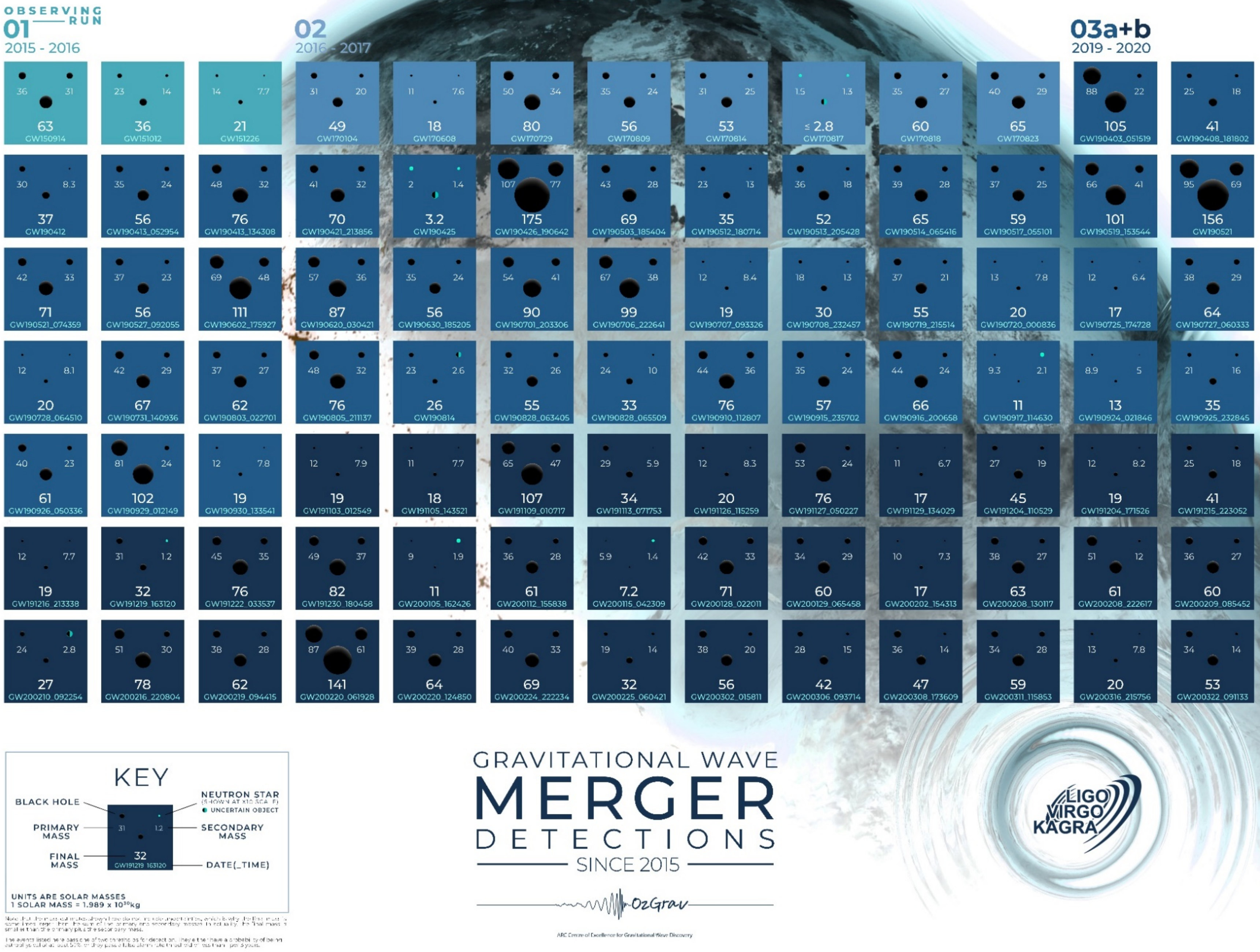
OBSERVING RUN
01 2015 - 2016
02 2016 - 2017
03a+b 2019 - 2020
36 31 63 GW150914
23 14 36 GW151012
14 7.7 21 GW151226
31 20 49 GW170104
11 7.6 18 GW170608
50 34 80 GW170729
35 24 56 GW170809
31 25 53 GW170814
1.5 1.3 ≤ 2.8 GW170817
35 27 60 GW170818
40 29 65 GW170823
88 22 105 GW190403_051519
25 18 41 GW190408_181802
30 8.3 37 GW190412
35 24 56 GW190413_052954
48 32 76 GW190413_134308
41 32 70 GW190421_213856
2 1.4 3.2 GW190425
107 77 175 GW190426_190642
43 28 69 GW190503_185404
23 13 35 GW190512_180714
36 18 52 GW190513_205428
39 28 65 GW190514_065416
37 25 59 GW190517_055101
66 41 101 GW190519_153544
95 69 156 GW190521
42 33 71 GW190521_074359
37 23 56 GW190527_092055
69 48 111 GW190602_175927
57 36 87 GW190620_030421
35 24 56 GW190630_185205
54 41 90 GW190701_203306
67 38 99 GW190706_222641
12 8.4 19 GW190707_093326
18 13 30 GW190708_232457
37 21 55 GW190719_215514
13 7.8 20 GW190720_000836
12 6.4 17 GW190725_174728
38 29 64 GW190727_060333
12 8.1 20 GW190728_064510
42 29 67 GW190731_140936
37 27 62 GW190803_022701
48 32 76 GW190805_211137
23 2.6 26 GW190814
32 26 55 GW190828_063405
24 10 33 GW190828_065509
44 36 76 GW190910_112807
35 24 57 GW190915_235702
44 24 66 GW190916_200658
9.3 2.1 11 GW190917_114630
8.9 5 13 GW190924_021846
21 16 35 GW190925_232845
40 23 61 GW190926_050336
81 24 102 GW190929_012149
12 7.8 19 GW190930_133541
12 7.9 19 GW191103_012549
11 7.7 18 GW191105_143521
65 47 107 GW191109_010717
29 5.9 34 GW191113_071753
12 8.3 20 GW191126_115259
53 24 76 GW191127_050227
11 6.7 17 GW191129_134029
27 19 45 GW191204_110529
12 8.2 19 GW191204_171526
25 18 41 GW191215_223052
12 7.7 19 GW191216_213338
31 1.2 32 GW191219_163120
45 35 76 GW191222_033537
49 37 82 GW191230_180458
9 1.9 11 GW200105_162426
36 28 61 GW200112_155838
5.9 1.4 7.2 GW200115_042309
42 33 71 GW200128_022011
34 29 60 GW200129_065458
10 7.3 17 GW200202_154313
38 27 63 GW200208_130117
51 12 61 GW200208_222617
36 27 60 GW200209_085452
24 2.8 27 GW200210_092254
51 30 78 GW200216_220804
38 28 62 GW200219_094415
87 61 141 GW200220_061928
39 28 64 GW200220_124850
40 33 69 GW200224_222234
19 14 32 GW200225_060421
38 20 56 GW200302_015811
28 15 42 GW200306_093714
36 14 47 GW200308_173609
34 28 59 GW200311_115853
13 7.8 20 GW200316_215756
34 14 53 GW200322_091133
KEY
BLACK HOLE
NEUTRON STAR
UNCERTAIN OBJECT
PRIMARY MASS
SECONDARY MASS
FINAL MASS
DATE(_TIME)
31 1.2 32 GW191219_163120
UNITS ARE SOLAR MASSES
1 SOLAR MASS = 1.989 x 10^30 kg
GRAVITATIONAL WAVE
MERGER
DETECTIONS
SINCE 2015
OzGrav
ARC Centre of Excellence for Gravitational Wave Discovery
LIGO
VIRGO
KAGRA